UNCLASSIFIED

AD NUMBER
AD475777
NEW LIMITATION CHANGE
TO **Approved for public release, distribution unlimited**
FROM **Distribution authorized to U.S. Gov't. agencies and their contractors; Critical Technology; 05 JAN 1965. Other requests shall be referred to Air Force Ballistic Systems Division, Missile Reentry Systems, Norton AFB, CA.**
AUTHORITY
samso usaf ltr 28 feb 1972

THIS PAGE IS UNCLASSIFIED

TECHNICAL OPERATING REPORT
BOB Approval Nr. 21-R136.1

475777

CONVECTIVE STAGNATION POINT HEATING FOR REENTRY SPEEDS UP TO 70,000 FEET/SECOND INCLUDING EFFECTS OF LARGE BLOWING RATES

(Task 3.1: Flow Field Analysis -- REST Program)

Prepared by

Philip DeRienzo

Adrian Pallone

RESEARCH AND DEVELOPMENT DIVISION
AVCO CORPORATION
Wilmington, Massachusetts

RAD-TM-65-58
Contract AF04(694)-498

THIS REPORT WAS PREPARED IN ACCORDANCE WITH AIR FORCE CONTRACT AF04(694)-498. IT IS SUBMITTED IN PARTIAL FULFILLMENT OF THE CONTRACT AND IN ACCORDANCE WITH AFBM EXHIBIT 58-1 (PARAGRAPH 3.18).

5 January 1965

Prepared for

BALLISTIC SYSTEMS DIVISION
DEPUTY FOR BALLISTIC MISSILE REENTRY SYSTEMS
AIR FORCE SYSTEMS COMMAND
Norton Air Force Base, California

TECHNICAL OPERATING REPORT
BOB Approval Nr. 21-R138.1

This document consists of 60 pages,
117 copies, Series A

CONVECTIVE STAGNATION POINT HEATING FOR REENTRY SPEEDS UP TO 70,000 FEET/SECOND INCLUDING EFFECTS OF LARGE BLOWING RATES

(Task 3.1: Flow Field Analysis -- REST Program)

Prepared by

Philip DeRienzo

Adrian Pallone

RESEARCH AND DEVELOPMENT DIVISION
AVCO CORPORATION
Wilmington, Massachusetts

RAD-TM-65-58
Contract AF04(694)-498

THIS REPORT WAS PREPARED IN ACCORDANCE WITH AIR FORCE CONTRACT AF04(694)-498. IT IS SUBMITTED IN PARTIAL FULFILLMENT OF THE CONTRACT AND IN ACCORDANCE WITH AFBM EXHIBIT 58-1 (PARAGRAPH 3.10).

5 January 1965

APPROVED

A. J. Pallone, Manager
Aerophysics Department

J. A. Lucori, Manager
REST Project Office

Prepared for

BALLISTIC SYSTEMS DIVISION
DEPUTY FOR BALLISTIC MISSILE REENTRY SYSTEMS
AIR FORCE SYSTEMS COMMAND
Norton Air Force Base, California

ABSTRACT

The current state-of-the-art is reviewed with respect to the calculation of convective stagnation point heating at supersatellite reentry speeds. Recently calculated transport properties have been compared with experiment. It is noted that theoretical and experimental estimates of the total thermal conductivity are in much closer agreement than reported by earlier investigators.

Similarity solutions employing these recently computed transport properties are presented for the convective heat transfer rate in an ionized, dissociated gas for equilibrium air and equilibrium nitrogen at reentry speeds up to 70,000 feet/sec. Solutions are also obtained for the case when large rates of injection are introduced at the stagnation point. Tables of boundary layer characteristics including profiles of temperature, velocity, and enthalpy are presented for the axisymmetric and two-dimensional stagnation point.

This task was initiated under the REST Program under the cognizance of Air Force Ballistic Systems Division; the major portion of the work, however, has been company supported.

CONTENTS

ILLUSTRATIONS

TABLES

NOMENCLATURE

C_p	specific heat at constant pressure
f	Blasius function, $\int_0 u/u_1 \, d\eta$
f_w	$= \rho_w v_w \sqrt{2\rho_w \mu_w (du_1/dx)_o}$, injection parameter
g	enthalpy ratio H/H_1
h	static enthalpy
H	total enthalpy
j	0, 1 for two-dimensional, axisymmetric respectively
N	$= \rho\mu/\rho_w \mu_w$, dimensionless ratio
Nu	Nussett number
p	static pressure
P	total pressure
Pr	Prandtl number
$\dot{q}$	heat transfer rate
r	normal distance from body axis
R_N	nose radius
Re	Reynolds number
T	temperature
u, v	local components of velocity
V_∞	flight velocity
x, y	curvilinear coordinates

NOMENCLATURE (Concl'd)

μ	viscosity
ρ	density
ζ	velocity ratio, u/u_1
β	$2\,\dfrac{d(\ln u_1)}{d(\ln \xi)}$, pressure gradient term
η	$= \dfrac{u_1 r_w^{\,j}}{\sqrt{2\xi}} \displaystyle\int_0 \rho\, dy$, transformed coordinate
ξ	$= \displaystyle\int_0 \rho_w \mu_w u_1 r_w^{\,j}\, dx$, transformed coordinate

SUBSCRIPTS

1	conditions at outer edge of boundary layer
w	conditions at body surface
o	conditions at stagnation point
∞	conditions in undisturbed region upstream of body shock
c	conditions of injected mass

I. INTRODUCTION

One of the immediate problems in the design of vehicles entering the Earth's atmosphere at supersatellite velocities is the determination of heat transfer from a stream containing dissociated and partially ionized gas. In order to attack this problem, one must know with a certain degree of accuracy the transport and thermodynamic properties, and the rate processes involved. A complete solution of the overall problem, where one takes into account body geometry and general ablating surfaces, is at present nonexistent. Specialized solutions are available, however. Examples are: simplified chemistry (i.e., equilibrium), simplified geometry (i.e., stagnation point), and simplified ablation (i.e., pseudo-binary mixture of air and ablated gas).

One of the earlier studies which accounted for the influence of electronic heat conduction at high temperatures was that of Adams[1] in which the frozen air boundary layer with a fully catalytic wall was treated. Adams' results, based on simplified transport properties, indicated that at entry speeds of 45,000 ft/sec, the convective heat transfer rate with ionization effects was 30 percent higher than convective heating without ionization obtained by extrapolation of existing theories.

To illustrate the significance of entry speeds, lunar probes reentry the Earth's atmosphere at 35,000 ft/sec while Mars probes reenter at 45,000 to 65,000 ft/sec. Air begins to ionize significantly at less than 10,000°K and is completely single-ionized at 20,000°K. At 50,000 ft/sec and altitude of 190,000 feet, the stagnation temperature is 15,000°K.

Van Tassell and Pallone[2], employing similarity-type solutions, used Hansen's[3] properties to study the heat transfer rate for air in equilibrium dissociation and ionization. Comparing their results and those of Adams with Avco RAD experimental results they found good agreement between theory and experiment for flight speeds up to 35,000 ft/sec. Cohen[4], also using similarity-type solutions and employing Hansen's properties, was able to show agreement with Van Tassell and Pallone for flight speeds up to 40,000 ft/sec.

A severe departure from the above-mentioned theory was obtained by Scala[5]. His results for equilibrium N_2 showed extremely high heat transfer rates. The transport properties used by Scala were based on a charge-induced dipole model for the species N_2, N, N^+, and e^-. Pallone and Van Tassell[6] compared transport properties computed from Yos[7] collision integrals based on the species, N_2, N, N^+, N^{++}, and e^- and were able to show discrepancies in Scala's high temperature model. These discrepancies are discussed in detail in reference 6 where theoretical predictions of thermal conductivity are compared with estimates of thermal conductivity derived from Maecker arc experiments.

Hoshizaki[8], using similarity-type solutions accounted for the effects of dissociation and ionization through the useful concept of total thermodynamic and transport property (i.e., reaction conductivity, first discussed by Hirshfelder, and subsequently used in reference 2). Hoshizaki employed Hansen's properties and obtained correlations applicable to an Earth or Venus atmosphere which agreed well with his own experimental heat transfer data. Comparison of the Hoshizaki correlation equation (equation 20 of reference 8) shows good agreement with the results of reference 2, 4, and 6, for flight speeds up to 40,000 ft/sec. Adams' results for a frozen boundary layer were also in good agreement with Hoshizaki.

Fay and Kemp[9] proposed a simplified binary diffusion model in which one diffusion equation as well as three overall conservation equations are used just as in the case of the dissociated gas boundary layer. This model is based upon an assumption that the relative velocity between the ions and atoms is negligible compared with other diffusion velocities. The justification proposed for this assumption is that the charge exchange cross section for $N \cdot N^+$ collisions (based on estimates by Yos[7]) is much greater than that for other heavy-particle collisions, thereby impeding the relative motion of the ions with respect to the atoms. The results of Fay and Kemp for equilibrium N_2 are in good agreement with those of Pallone and Van Tassell over a large velocity range.

The comprehensive experimental results of Rose and Stankevics[10] using the electrical driven shock tube confirmed the conclusions of Pallone and Van Tassell and the theoretical results of Fay and Kemp for equilibrium N_2 in addition to verifying the theories of Cohen and Hoshizaki for equilibrium air. The agreement between theory and experiment was thus fairly well established for flight speeds up to 50,000 ft/sec.

Attaining equivalent flight speeds substantially higher than 50,000 ft/sec in the shock tube has proven difficult so that sufficient experimental verification of heat transfer rates is generally not available for the very high speed flight regime. Furthermore, uncertainties in calculating the total thermal conductivity for partially ionized air have discouraged previous efforts to extend theoretical predictions of stagnation point heat transfer to flight speeds above 50,000 ft/sec.

Howe and Schaeffer[11] have examined the effects of uncertainties in the total thermal conductivity of air on convective heat transfer for stagnation temperature up to 30,000°K. Using a merged shock-layer type of solution they employed the following variations of Yos' [7], transport properties: (1) Yos' thermal conductivity of reference 7, (2) Yos' thermal conductivity increased by an order of magnitude at the high temperature end, and (3) Yos thermal conductivity faired into Hansen's thermal conductivity at 13,000°K. Their

results indicate that the convective heat transfer rate is relatively insensitive to large uncertainties in the total thermal conductivity. For example, an uncertainty of a factor of 10 in the total thermal conductivity of air influences the convective heating rate by only a factor of 1.75 at a flight velocity of 70,000 ft/sec. and by a factor of 2 at 85,000 ft/sec. This effect has also been shown in reference 6, where a comparison was made of the heat transfer rate using Maecker's arc data and Yos' theoretical data.

The object of the present report is to extend the equilibrium air analytical study of Pallone and Van Tassell[6] to flight speeds up to 70,000 ft/sec. For the present study we employ the most recent transport and thermodynamic properties calculated by Yos[12], and examine the stagnation point convective heat transfer. Results are then compared with experiment, including recent Avco RAD shock tube data [13]. Boundary layer profiles for both two-dimensional and axisymmetric bodies are included in this report. Results are also presented showing first order effects of simulated ablation, i.e., pseudo-binary mixture of air and injected air.

The effects of blowing on the convective heat transfer has been the subject of many studies, including those of Reshotko and Cohen[14] who used constant-property boundary layer solutions. Libby[15] relaxed these restrictions on the thermodynamic and transport properties by taking the properties as simple functions of the temperature. The results of both studies, however, are applicable only to very low flight speeds because of the choice of transport properties. Of special note is an excellent report by Howe and Schaeffer[16] which employs variable transport and thermodynamic properties with a merged-layer-type solution to study stagnation point flows for flight velocities between 30,000 and 50,000 ft/sec. Coupled radiative and convective heat transfer is presented as well as a comprehensive study of the effects of moderate rates of injection. In the present paper, the effects of blowing to show first-order effects of ablation are examined at flight speeds up to 65,000 ft/sec by extending the calculations for the convective heat transfer rate to include large rates of air injection at the stagnation point. Both two-dimensional and axisymmetric bodies are studied.

II. THERMODYNAMIC AND TRANSPORT PROPERTIES

Thermodynamic and transport properties calculated by Yos[7] and used in the analysis of Pallone and Van Tassell[6] have been superseded by Yos[12]. These new properties, which are employed in the present report, are shown in figures 1 to 8.

The new thermodynamic properties are very slightly changed as a result of Yos' new calculations. For example, the specific heat for air is only 5 to 15 percent higher at temperatures above 15,000°K. A comparison of Yos' new thermodynamic properties with those presented in AEDC-TR-64-183 (September 1964) showed excellent agreement for temperatures up to 15,000°K, which is as high as the AEDC tables go.

Significant changes are indicated, however, in the transport properties of figures 1 to 6, especially for the region of partial ionization. At 14,000°K, for example, the total thermal conductivity for nitrogen is approximately 50 percent higher than Yos' earlier predictions in reference 7.

Theoretical calculations of transport properties are based on kinetic theory. That is, explicit formulas for viscosity and thermal conductivity as functions of collision integral, particle mass, and mol fraction of particular species are obtained from the first Chapman-Enskog approximation, or slight variation thereof (see Yos [7]).

For temperatures up to 10,000°K, the transport properties can be predicted with fairly good accuracy so that reasonable agreement exists among various investigators. However, above 10,000°K, where partial ionization exists, there has been considerable disagreement in the prediction of the total thermal condictivity. Total thermal conductivity, which appears in the definition of the Prandtl number, $Pr = \mu C_p/k$, includes the effects of ordinary translational energy transport, thermal diffusion, and chemical and ionization reactions.

In the region of partial ionization (9,000 to 16,000°K) resonant charge-exchange processes in which an electron is transferred from an atom to a positive ion of the same species (e.g., $N + N^+ \rightarrow N^+ + N$) are a major component of the thermal conductivity of the gas. By including the effects of charge-exchange Yos[7] obtained a diffusion cross section between atoms and atomic ions which was almost an order of magnitude larger than the gas-kinetic cross section used in most previous high temperature transport property calculations.

The most recent calculations by Yos[12] yield charge-exchange cross sections for oxygen which are in excellent agreement with the experimental measurements of Stebbings, et al.[12] No experimental cross sections have yet been measured for nitrogen but Yos' recent theoretical cross sections for nitrogen appear to be in fair agreement with the recent semiemperical estimates of

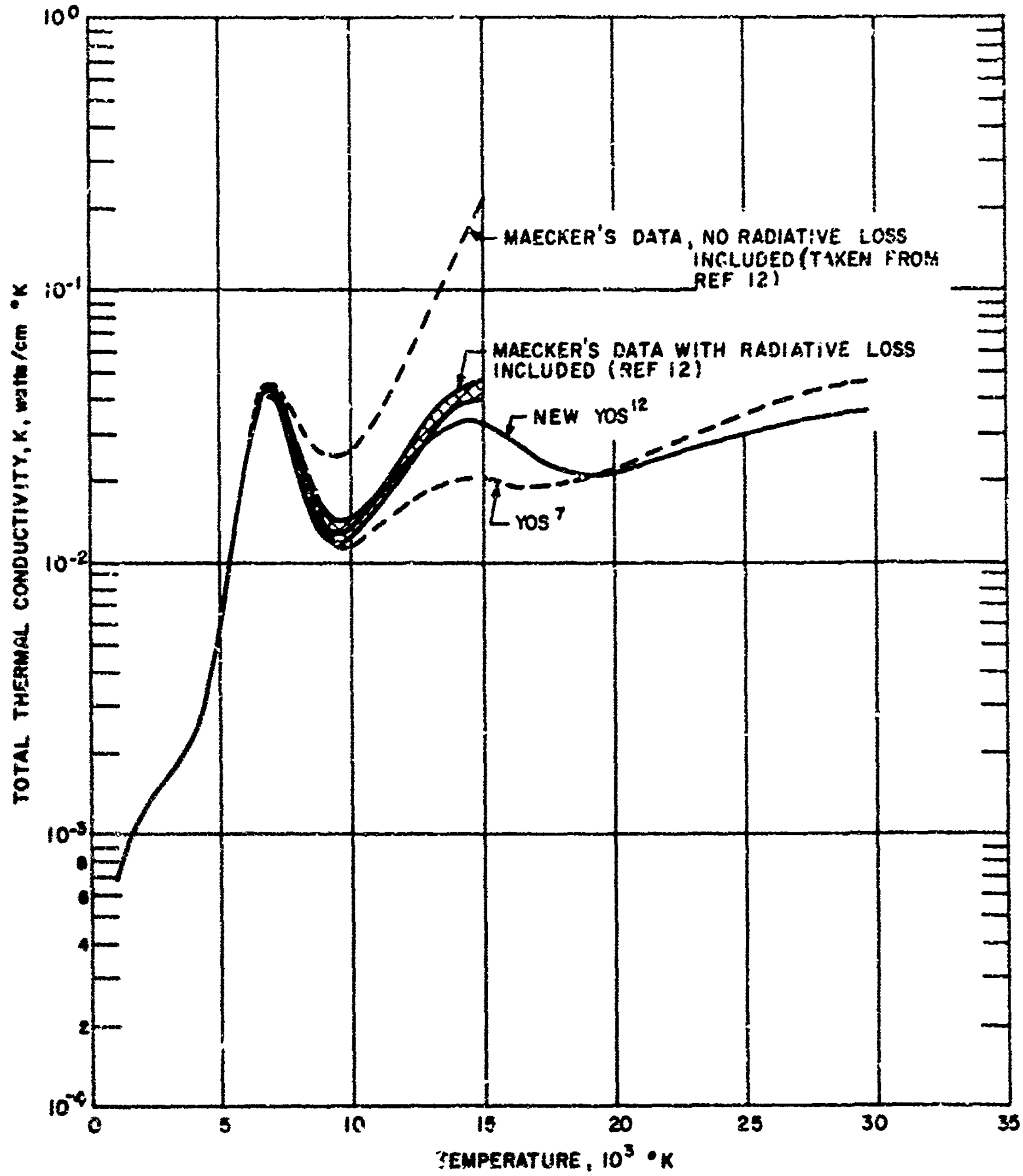

85-5481

Figure 1 TOTAL THERMAL CONDUCTIVITY FOR EQUILIBRIUM NITROGEN AT ATMOSPHERE PRESSURE

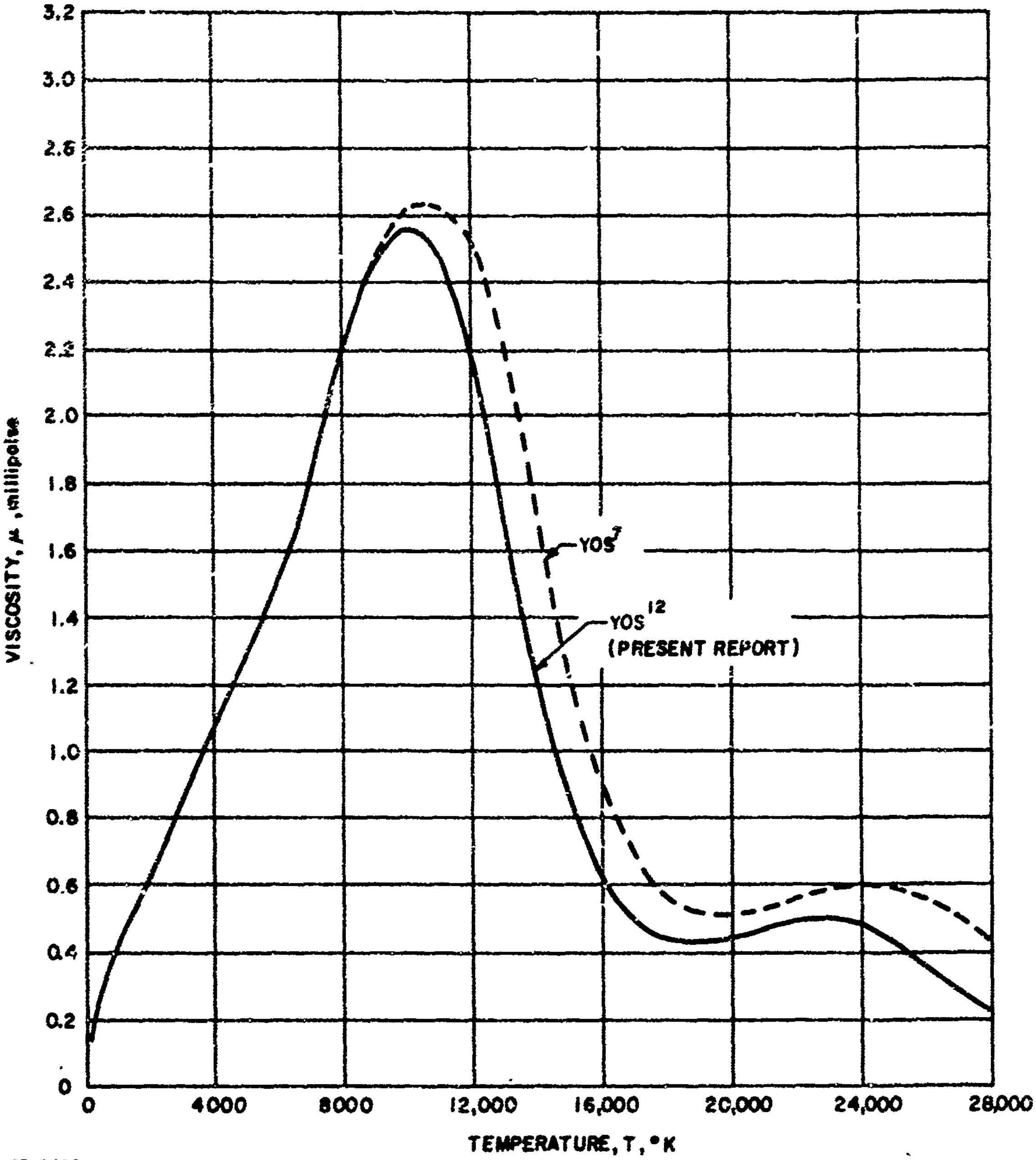

65-5482

Figure 2 VISCOSITY OF EQUILIBRIUM NITROGEN, N_2, AT P = 1 ATMOSPHERE

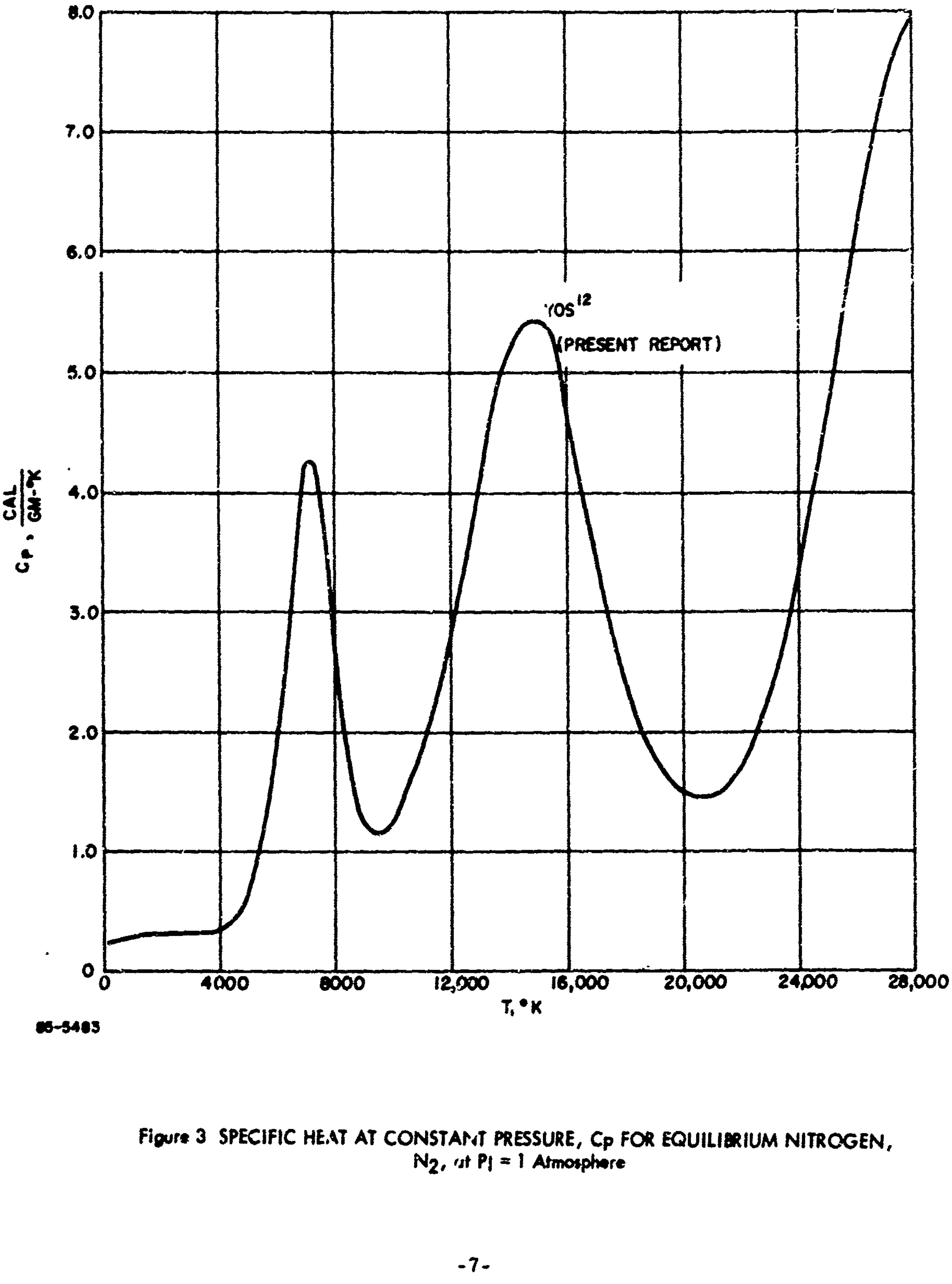

Figure 3 SPECIFIC HEAT AT CONSTANT PRESSURE, Cp FOR EQUILIBRIUM NITROGEN, N_2, at P_1 = 1 Atmosphere

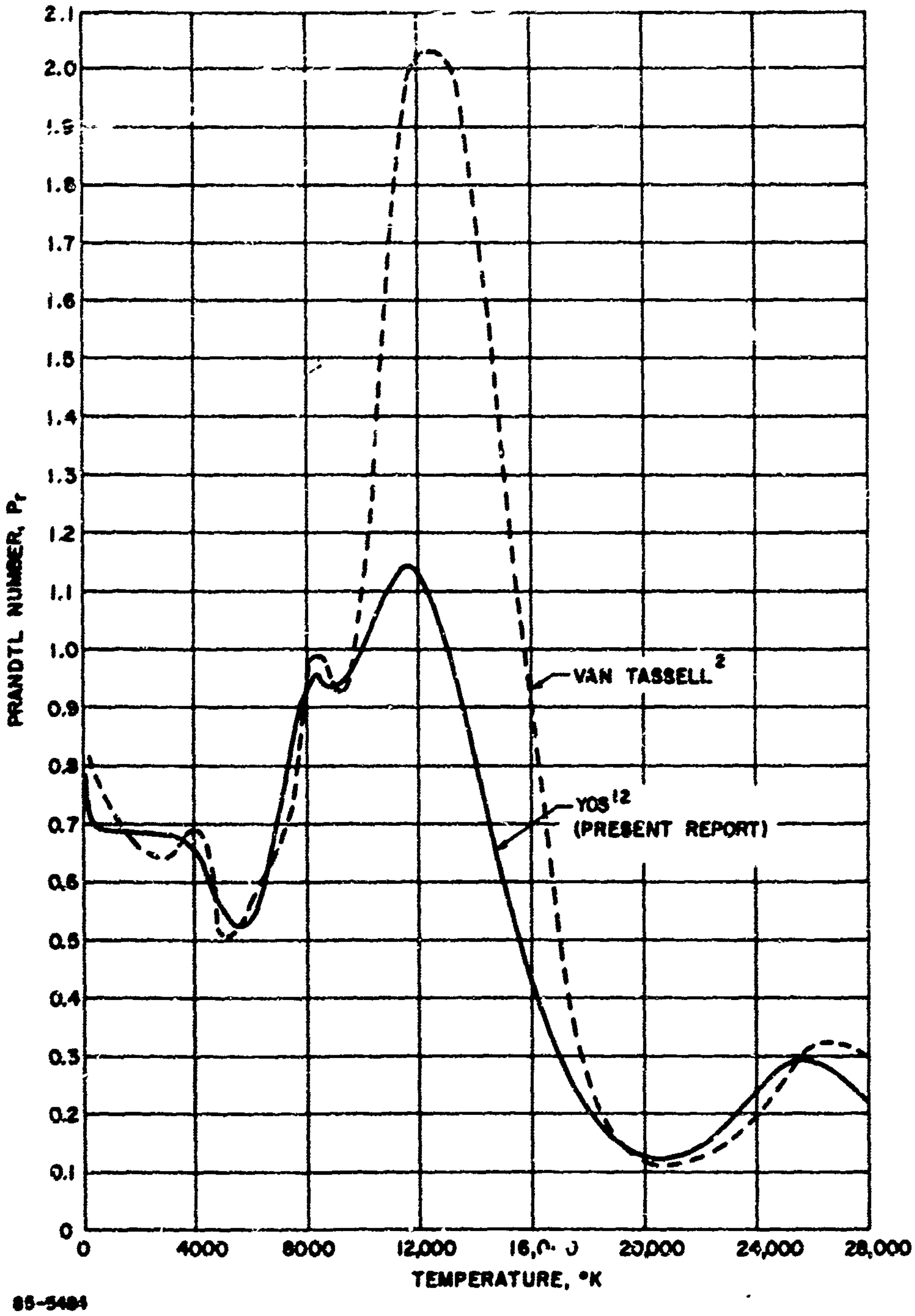

85-5484

Figure 4 PRANDTL NUMBER FOR EQUILIBRIUM NITROGEN, N_2, AT P_1 = 1 ATMOSPHERE

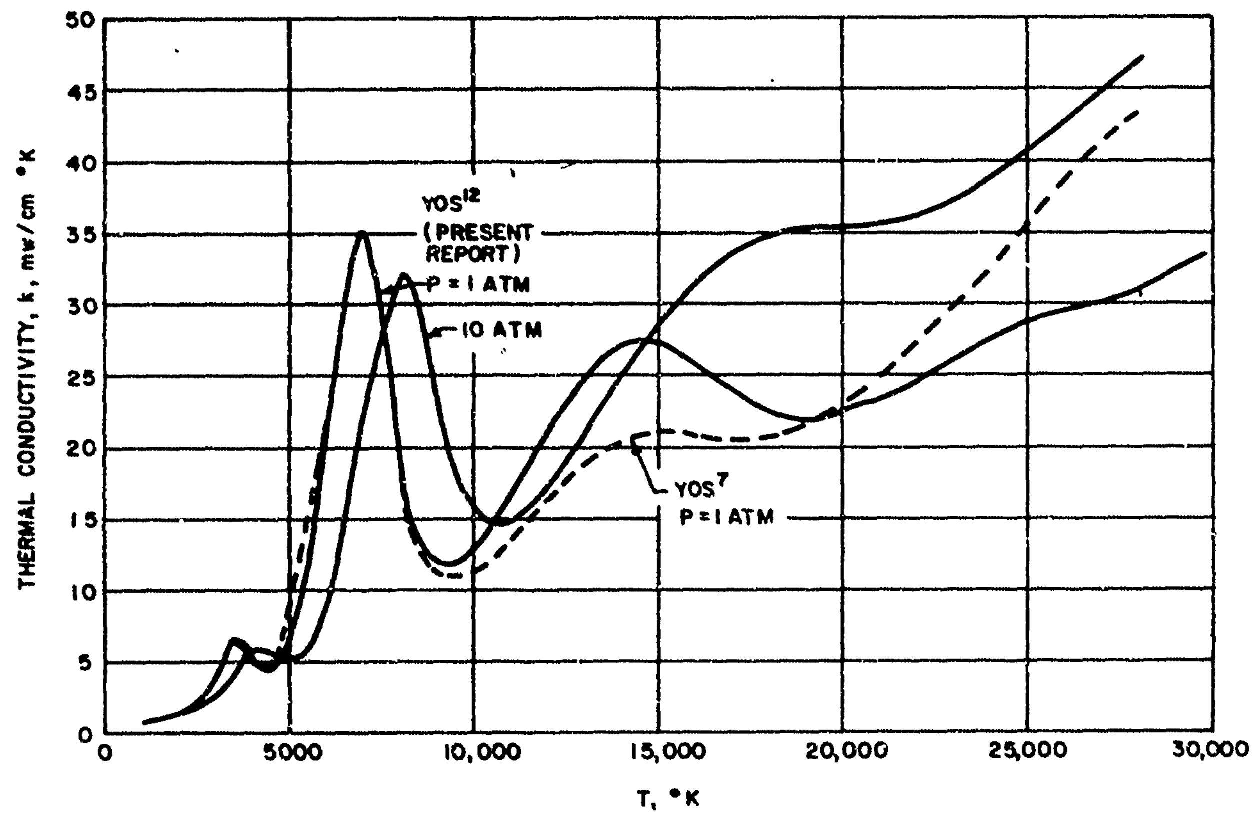

85-5485

Figure 5 TOTAL THERMAL CONDUCTIVITY FOR EQUILIBRIUM AIR

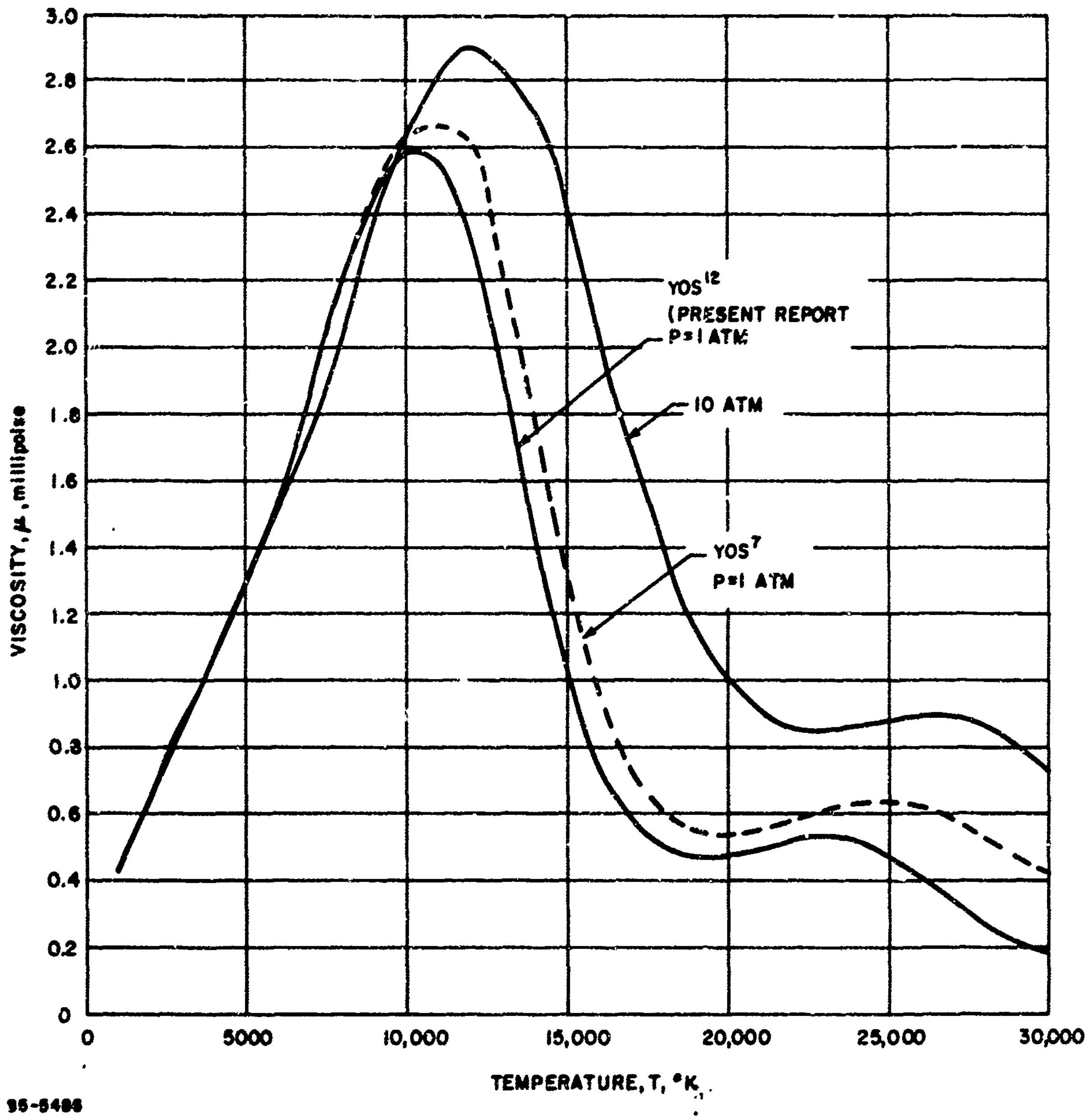

95-5486

Figure 6 VISCOSITY OF EQUILIBRIUM AIR

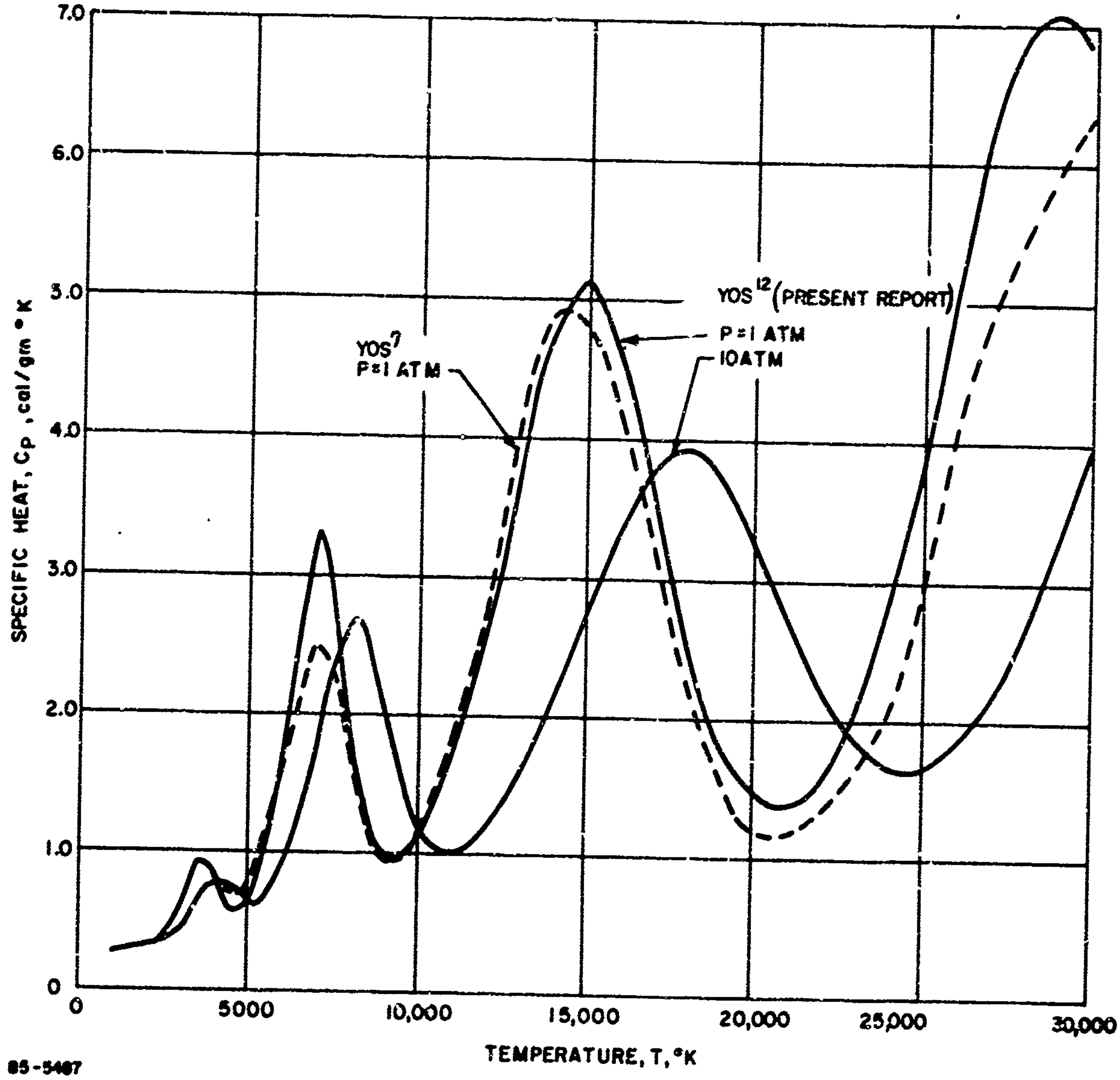

Figure 7 SPECIFIC HEAT AT CONSTANT PRESSURE FOR EQUILIBRIUM AIR

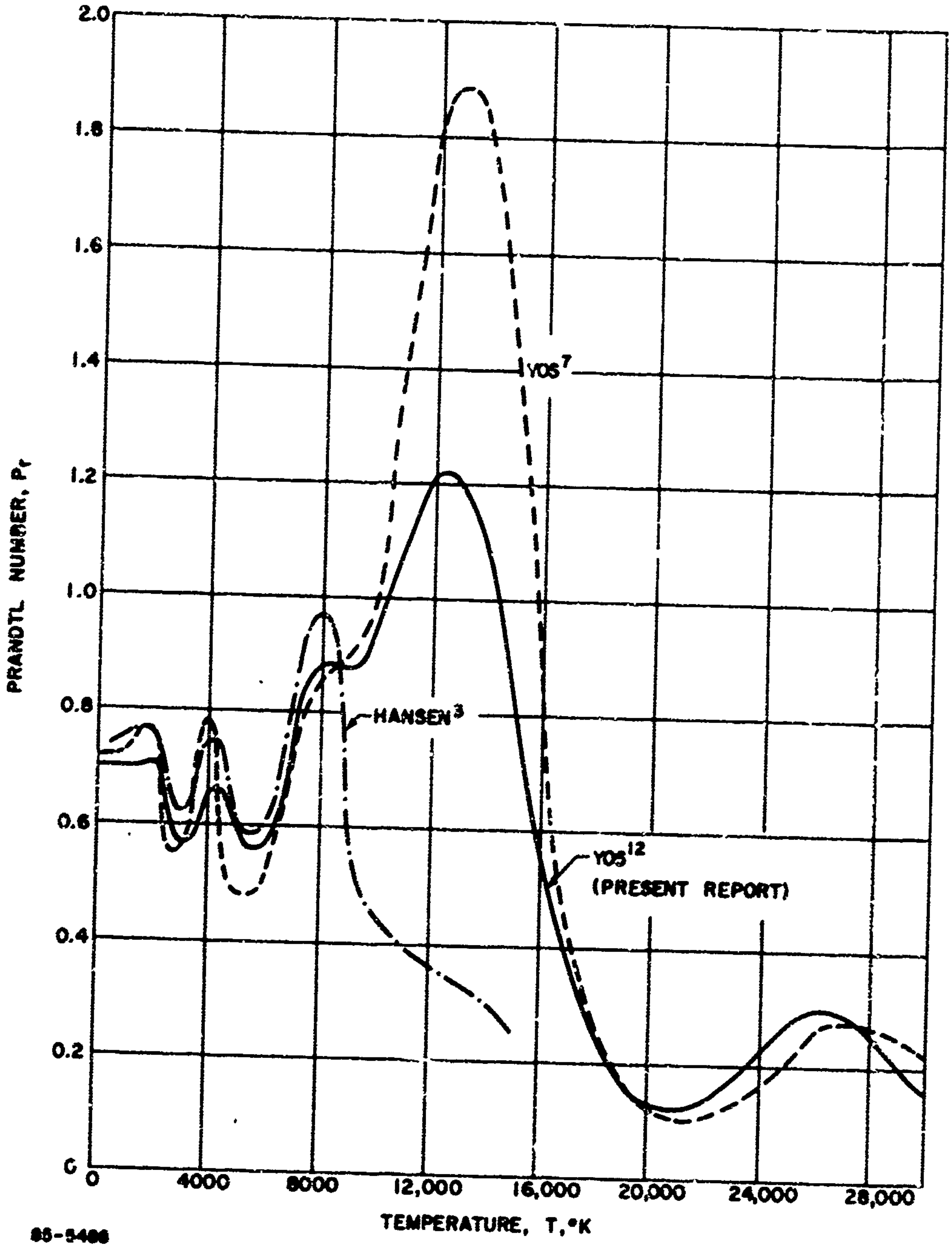

Figure 8 PRANDTL NUMBER FOR EQUILIBRIUM AIR AT P_1 = 1 ATMOSPHERE

Knof, Mason, and Vanderslice[12]. Yos' new nitrogen cross section results in a calculated thermal conductivity which is about 50 percent higher than his previous calculations, at the regions of interest here. This new prediction of thermal conductivity for nitrogen is also in good agreement with that of Ahtye for temperatures up to 15,000°K. (See reference 18.)

Experimental verification of thermal conductivity can be made using two general techniques. The first, and most commonly used technique, employs the constricted laminar arc-column originated by Maecker[19]. Using the constricted arc Maecker was able to determine total thermal conductivity for nitrogen at atmospheric pressure and temperatures from 5000 to 15,000°K. The second experimental technique employs overall heat transfer measurement in a shock tube from which one then infers the values of the total thermal conductivity.

With the first technique, the Elenbaas-Heller equation for radial energy transport in an optically-thin cylindrical arc column

$$\sigma E^2 + \frac{1}{r}\left[\frac{d(rK)}{dr}\ \frac{dT}{dr}\right] - P_{rad} = 0 \tag{1}$$

is integrated once and solved for the thermal conductivity K, at a radial distance r',

$$(K)_{r'} = -\frac{\int_0^{r'} (\sigma E^2 - P_{rad})\, r\, dr}{r\left(\frac{dT}{dr}\right)_{r'}} \tag{2}$$

where E is the electric field strength in the column, r is the radius of the constricting tube. σ is the electrical conductivity of the gas, and P_{rad} is the power radiated from the gas per unit volume. The gas properties σ, K, and P_{rad} are generally functions of the gas temperature T, as well as of the nature of the gas and the pressure. The general procedure of the measurement is to first determine the electrical conductivity $\sigma(T)$ from the integrated form of Ohm's law, using measured values of E, I, and the radial temperature distribution $T(r)$ for several different arc currents. The temperature profiles are obtained from continuum and line radiation. In the final step, the thermal conductivity $K(T)$ is obtained from equation (2) using the previously determined value of $\sigma(T)$ and the measured value of P_{rad}. Further details of this experimental technique are given in reference 12.

Additional experiments to determine the thermal conductivity of gases at elevated temperatures using the constricted arc column have been carried out at Avco RAD by Bennett, Yos, Knopp, Morris, and Bade[12].

Initial arc data obtained by the above researchers confirmed Maecker's experimental values for nitrogen at 5000 to 15,000°K. This experimental arc data when used with the Ellenbaas-Heller energy balance (equation (1), valid for optically thin gas) resulted in values of thermal conductivity at the higher temperatures which were greater by an order of magnitude than Yos[12] predictions. However, the experimental values were open to question since the experimental thermal conductivity is an apparent function of arc current. This observation suggested to Bennett, et al, that some energy transport mechanism might be present which had not been allowed for in the reduction of the data.

A systematic analysis of the data and careful research on the absorption coefficient of argon and nitrogen in the vacuum ultraviolet led to the conclusion that the arc column emits significant radiation in the far ultraviolet and is relatively opaque to such radiation for pressures on the order of one atmosphere. This finding suggested that the assumption of an optically-thin gas column is not applicable for use in the E-H energy balance.

When the vacuum ultraviolet radiation was included in an approximate manner in the assumed radiative loss for the analysis with nitrogen, the dependence of thermal conductivity on arc current was eliminated. Furthermore, the experimental values were now found to be in good agreement with Yos' predictions, as can be seen from figure 1. However, before one can draw final conclusions the experimental thermal conductivity should be obtained from solutions of the E-H equation with nongray radiative transfer terms.

To get a quantitative understanding of the effect of thermal conductivity on the heat transfer rate, boundary layer solutions were obtained using the four thermal conductivity curves shown in figure 9. For each boundary layer solution the values for μ and C_p were taken from figures 2 and 3, respectively.

Figure 10 shows dramatically the effect of thermal conductivity on the heat transfer rate. In comparing the temperature profiles for the above cases it is interesting to note that the heat transfer rate is controlled primarily by conductivity in the vicinity of the wall. The dip in the thermal conductivity for the temperature region 7000 to 9000°K produces the effect of a relatively insulating layer which divides the boundary layer into two regions, a high temperature outer layer, and a lower temperature inner layer. Values of heat transfer rate tabulated in figure 10 also give evidence that this apparent layer of relatively low conductivity gas effectively insulates the body surface from the high temperature gases which exist at the edge of the boundary layer.

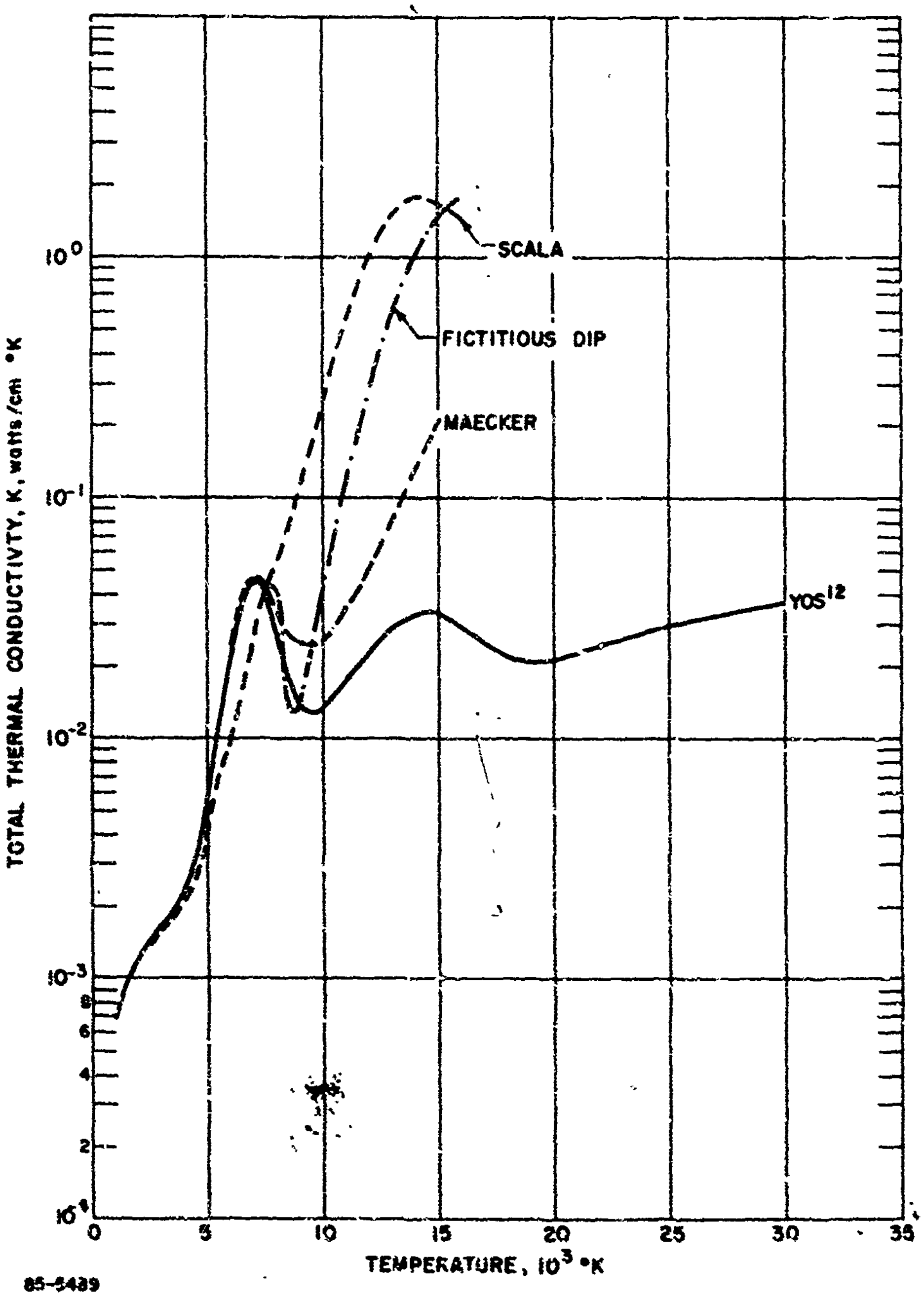

Figure 9 TOTAL THERMAL CONDUCTIVITY FOR EQUILIBRIUM NITROGEN AT ONE ATMOSPHERE PRESSURE

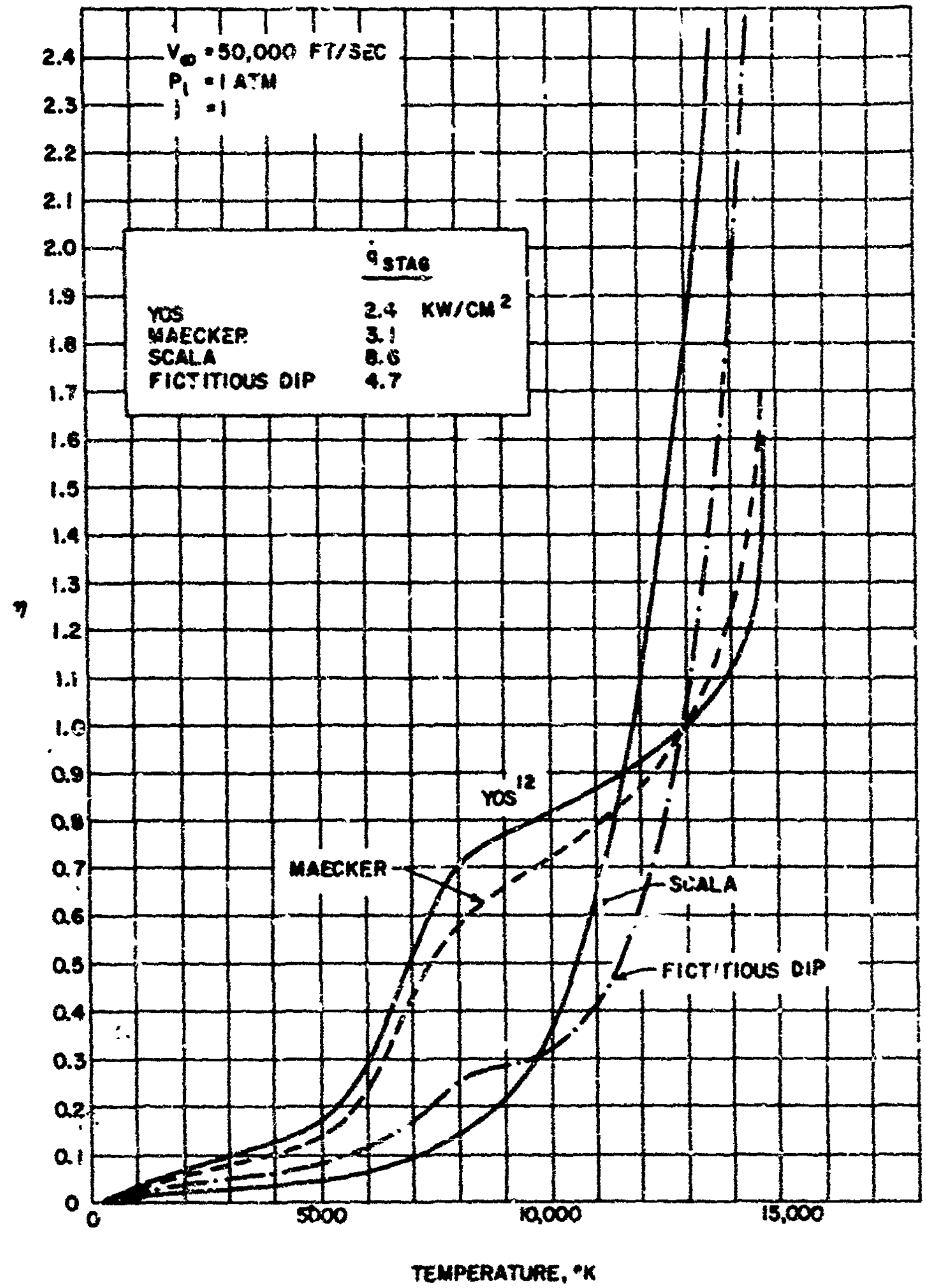

85-5490

Figure 10 TEMPERATURE PROFILES FOR EQUILIBRIUM NITROGEN

III. ANALYSIS

The well-known boundary layer equations describing the two-dimensional and axisymmetric flow of a gas in equilibrium dissociation and ionization are given below. The effect of diffusion is contained in the reaction conductivity which, in turn, is contained in the Prandtl number. Transverse curvature and pressure diffusion effects have been neglected.

Continuity equation

$$\frac{\partial}{\partial x}(\rho u r^j) + \frac{\partial}{\partial y}(\rho v r^j) = 0 \tag{3}$$

Momentum equation in x-direction

$$\rho u \frac{\partial u}{\partial x} + \rho v \frac{\partial u}{\partial y} = -\frac{\partial p}{\partial x} + \frac{\partial}{\partial y}\left(\mu \frac{\partial u}{\partial y}\right) \tag{4}$$

Energy equation

$$\rho u \frac{\partial H}{\partial x} + \rho u \frac{\partial H}{\partial y} = \frac{\partial}{\partial y}\left(\frac{\mu}{Pr}\frac{\partial H}{\partial y}\right) + \frac{\partial}{\partial y}\left\{\mu\left(1 - \frac{1}{Pr}\right)\frac{\partial (u^2/2)}{\partial y}\right\} \tag{5}$$

Input tables of thermodynamic properties are employed in the present analysis in place of the equation of state. In addition, the analysis of the injection region can be made of practical interest by adding the heat balance relation,

$$\left(K \frac{\partial T}{\partial y}\right)_w = (\rho v)_w (h_w - h_c) \tag{6}$$

Introducing the Levy-Lees transformation and the concept of local similarity, the above equations reduce to the following form:

$$[N f_{\eta\eta}]_\eta + f f_{\eta\eta} + 2\,\frac{d\,ln\,u_1}{d\,ln\,\xi}\left[\frac{\rho_1}{\rho} - f_\eta^2\right] = 0 \tag{7}$$

$$\left[\frac{N}{Pr} g_\eta\right]_\eta + f g_\eta + \frac{u_1^2}{H_1}\left[\left(1 - \frac{1}{Pr}\right) N f_\eta f_{\eta\eta}\right]_\eta = 0 \tag{8}$$

where,

$$N = \frac{\rho\mu}{\rho_w \mu_w} \; ; \; \xi = \int_0^x \rho_w \mu_w u_1 r^{2j} \, dx$$

$$\eta = \int_0^y \frac{u_1 r^j}{\sqrt{2\xi}} \rho dy \; ; \; f = \int_0^\eta \frac{u}{u_1} d\eta \; ; \; g = \frac{H}{H_1}$$

The appropriate boundary conditions for these equations are:

$$\text{At} \quad \eta = 0: \quad f = f(0) = -\frac{\rho_w v_w \sqrt{2\xi}}{\rho_w \mu_w u_1 r^j} \; ; \; f_\eta = 0$$

$$\text{At} \quad \eta \to \infty: \quad f_\eta \to 1 \; ; \quad g \to 1$$

In addition, if the energy balance is required as an optional boundary condition, the following equation holds,

$$\frac{[g_\eta]_w}{g_w - g_c} = -\,Pr_w\, f(0) \tag{9}$$

If there is no injection, or if the use of an energy balance is not desired, then either g_w or $[g_\eta]_w$ is given and the remaining boundary values are found in the solution.

DESCRIPTION OF PROGRAM

Particular solutions to equations (7), (8) and (9) were obtained by employing the iterative integration method described in detail by Van Tassell and Pallone [2]. In this scheme, an additional transformation is introduced which reduces the above system of ordinary differential equations to a set of five first-order differential equations which are then solved by an iteration procedure employing 1000 points across the boundary layer. The Prandtl number and $\rho\mu$ ratio are allowed to vary continuously, and convergence is very rapid. A typical boundary layer solution requires approximately one-half minute of machine time with usually less than 10 iterations per case.

IV. RESULTS AND DISCUSSION

Boundary layer characteristics (including velocity and temperature profiles, and heat transfer rates) were computed at the stagnation point for a spherical and cylindrical body with a radius of one foot and a representative stagnation pressure of one atmosphere and 10 atmospheres. The calculations covered the range of flight speeds from 5000 to 70,000 ft/sec. Values of the blowing parameter, $-f_w$, included 0.0, 0.25, 0.50, and 1.0. The injected fluid was assumed to be equilibrium air.

Table I summarizes the results for the cases studied in this report. The boundary layer profiles for these cases are given in tables II through VII. For laminar boundary layers it is well known that $\dot{q}$ varies with the square root of the pressure P_1. Since the transport properties are known to exhibit a very weak dependence on pressure, it follows that the heat transfer rates of table I can be scaled for arbitary stagnation pressures. Typically, such scaling would be valid for a Mars reentry trajectory where stagnation pressures may vary from 0.01 atmosphere to several atmospheres.

It may be noted in table I that when blowing is present, and in particular if f_w is kept constant, then $\dot{q}$ as a function of flight speed will go through a maximum. This peculiar behavior of $\dot{q}$ should not be interpreted in the practical sense that $\dot{q}$ will decrease for constant blowing with increasing V_∞. Rather, this behavior in $\dot{q}$ is a result of our definition of f_w and of the constraint that P_1 remain constant with increasing V_∞. If one defines the blowing parameter as $f_1 = -(\rho v)_w/\sqrt{2\rho_1\mu_1(du_1/dx)_o}$ so that $\rho\mu$ is evaluated at conditions at the edge of the boundary layer, rather than at the wall as is done in this report, then $\dot{q}$ will increase monotonically with increase in V_∞.

The calculated heat transfer rates for zero blowing are presented in figure 11 for comparison with recent shock tube measurements. Since we are interested mainly in the flight regime above 40,000 ft/sec the numerous theoretical results cited in the literature which are applicable to flight speeds below 40,000 ft/sec have not been included. It may be noted, however, that Hoshizaki's correlation equation for equilibrium air (equation 20 of reference 8) based on Hansen's transport properties would lie somewhat below our curve at V_∞ = 20,000 ft/sec and would intersect our curve at V_∞ = 44,000 ft/sec.

For clarity, only the curve fits from Rose and Stankevics[10] are shown in figure 11 although their curve fits represent a considerable number of data points extending up to equivalent flight speeds of 50,000 ft/sec.

The Avco RAD shock tube data shown in figure 11 indicates that shock velocities very near 13 mm/μsec (equivalent flight velocity of 56,000 ft/sec) are now being attained in the electrical driven shock tube. At the flight speeds above 50,000 ft/sec. the Avco RAD experimental data falls slightly above our

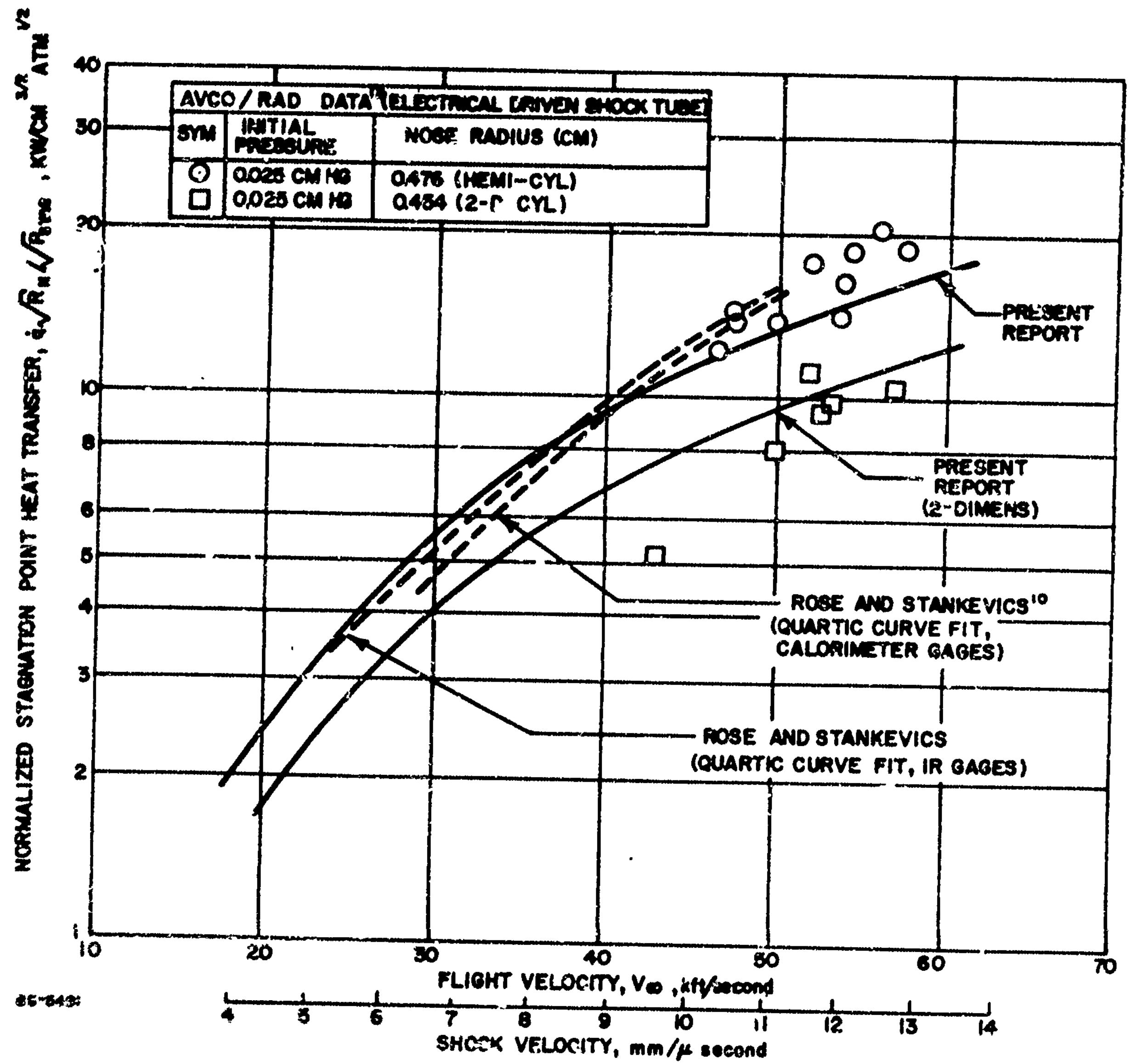

Figure 11 COMPARISON OF THEORETICAL PREDICTIONS WITH SHOCK TUBE DATA FOR NITROGEN WITH ZERO BLOWING

calculated results. Because the test models have a relatively small nose radius it seems unlikely that radiation from the surrounding gas cap could be significant at the prevailing test conditions. It is possible, however, that the model may be seeing ultraviolet radiation from the slug of test gas. Experiments are currently in progress to accurately determine the relative contributions due to radiation from the slug of test gas and from the surrounding gas cap.

The stagnation point velocity gradient used in the calculation of heat transfer rate for the two-dimensional bodies was based on Newtonian theory[20] and was calculated to be approximately 6 percent larger than the stagnation point velocity gradient for an axisymmetric body. This value for the two-dimensional body has been verified experimentally by Korkan[21].

Theoretical predictions of the convective heat transfer rate for equilibrium nitrogen are shown in figure 12 and compared with recent Avco RAD shock tube data. The agreement is excellent at flight speeds between 30,000 and 40,000 ft/sec. Not enough data is available at the flight speeds above 50,000 ft/sec to clearly show the trends indicated in the experimental data of figure 11. Theoretical heat transfer rates calculated by Fay and Kemp[9] using a simplified binary diffusion model are shown in figure 12 to be only slightly higher than those obtained in the present report. It can still be said, however, that in figure 12 the agreement between both theories and experiment is very good.

Results obtained for axisymmetric bodies using a pseudo-binary mixture of air and injected air are plotted in figure 13. The effect of the blowing parameter is seen to be seen to be strongly nonlinear at the higher blowing rates.

In order to obtain a quantitative understanding of the effect of transport properties on the heat transfer rates comparisons have been made with previous investigators as shown in figure 14. The results of Reshotko and Cohen[14] for a constant-property boundary layer are shown for two different temperature ratios. When the constant-property restriction is relaxed slightly, as for example, in the result shown for Libby[15] where the transport and thermodynamic properties are taken as simple functions of the temperature, then the heat transfer parameter $Nu/\sqrt{Re}$ is reduced. When the exact thermodynamic and transport properties are used, figure 14 shows that the level of $Nu/\sqrt{Re}$ is even further reduced, and in addition, a velocity dependence is introduced.

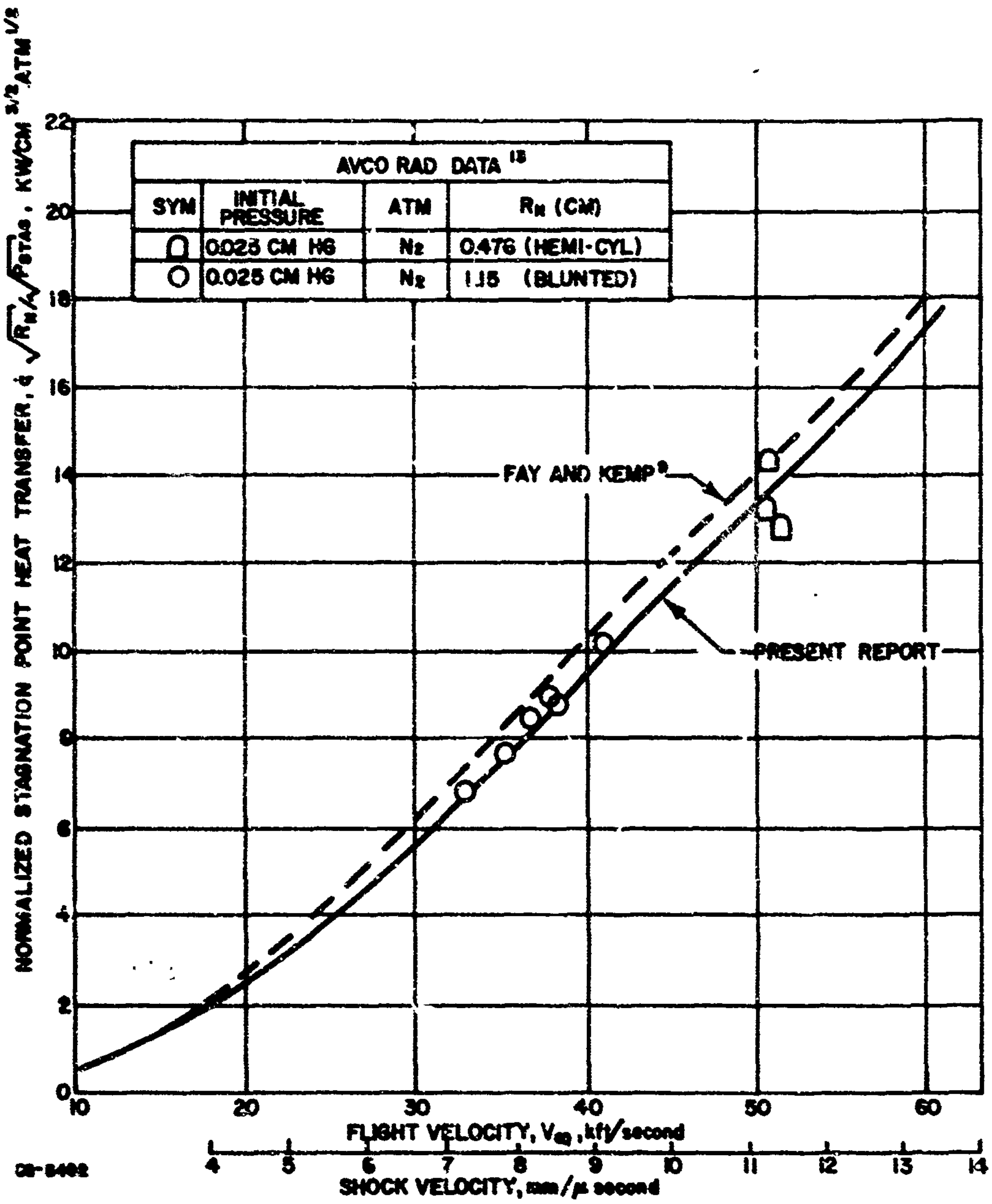

Figure 12 COMPARISON OF THEORETICAL PREDICTIONS WITH SHOCK TUBE DATA FOR NITROGEN WITH ZERO BLOWING

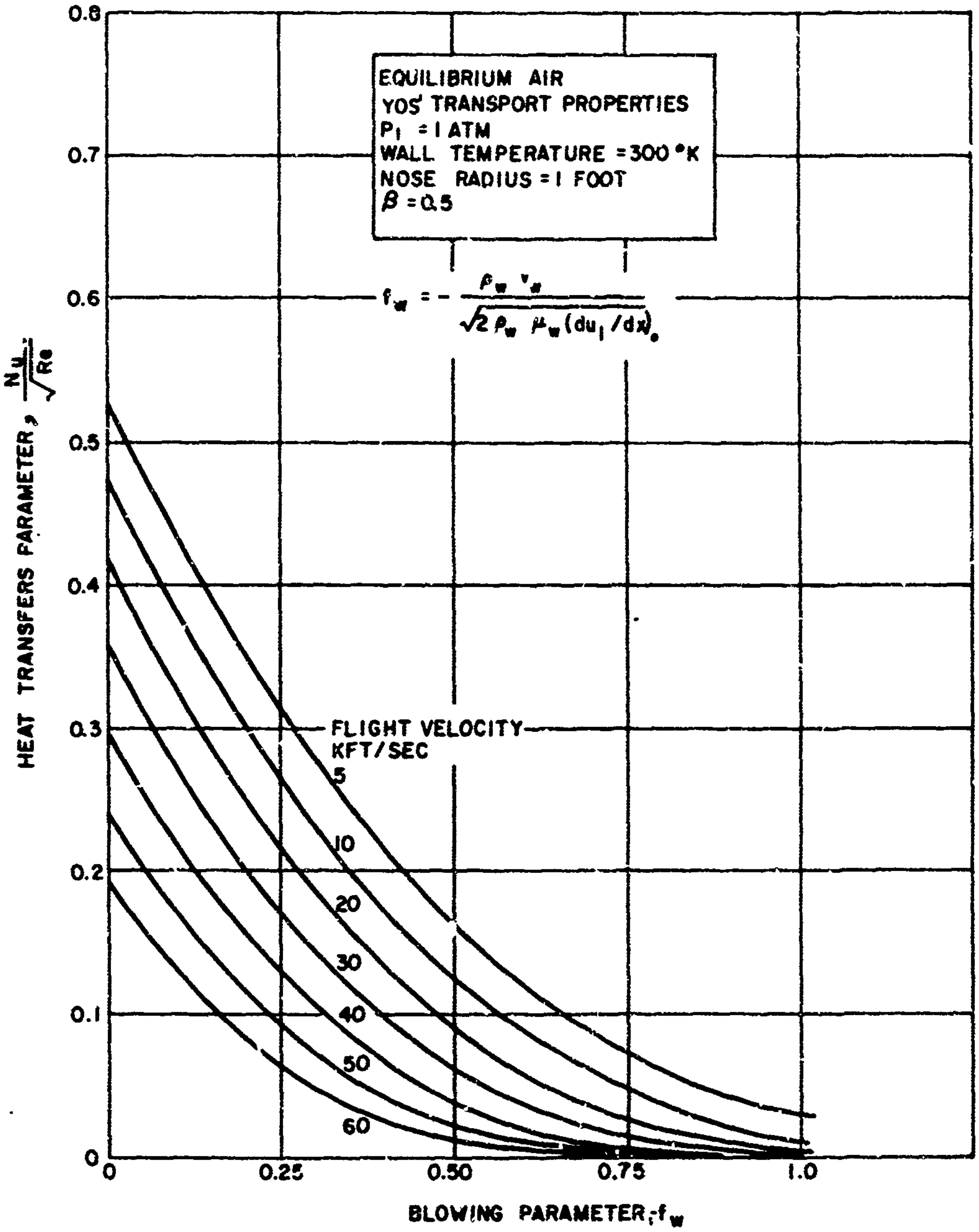

65-5493

Figure 13 EFFECT OF BLOWING ON THE HEAT TRANSFER PARAMETER AT THE STAGNATION POINT OF AN AXISYMMETRIC BLUNT BODY (AIR-AIR)

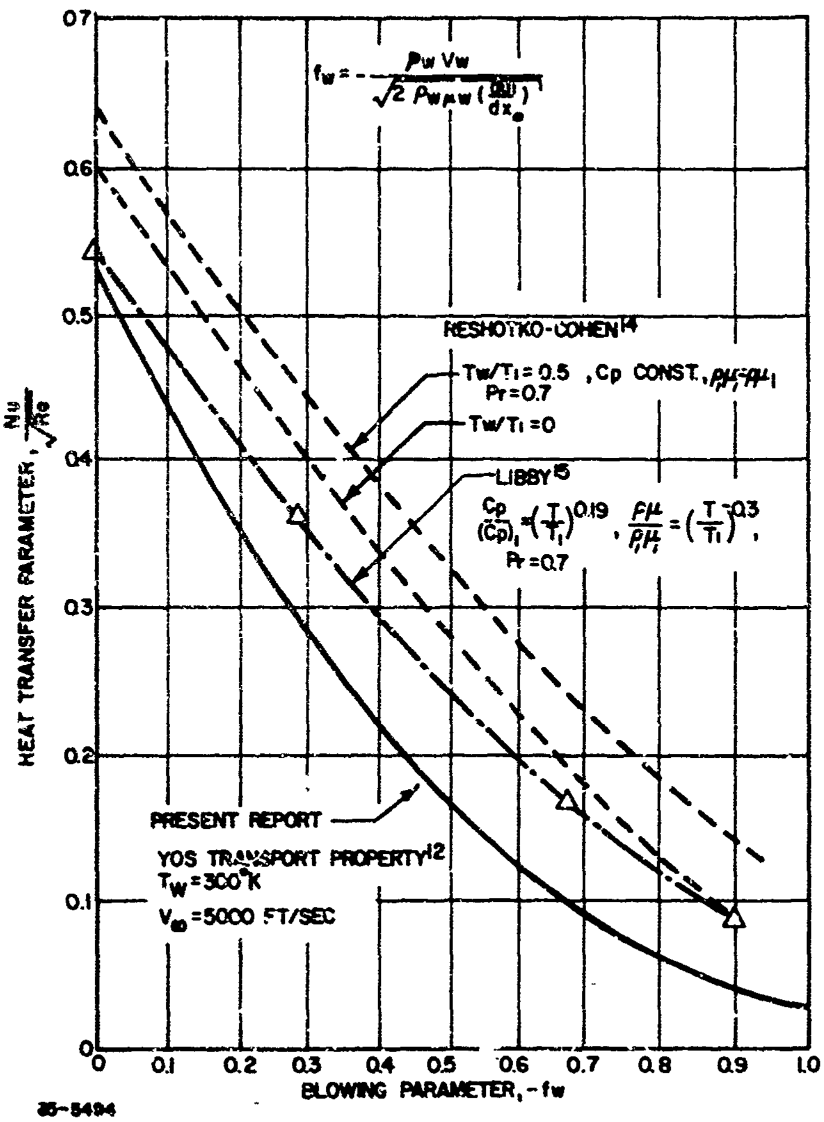

Figure 14 COMPARISON OF RESULTS SHOWING VARIATION OF NUSSELT NUMBER WITH BLOWING AT THE STAGNATION POINT OF AN AXISYMMETRIC BLUNT BODY (AIR-AIR)

TABLE I

SUMMARY OF RESULTS FOR EQUILIBRIUM AIR

	ATM			KFT/SEC		BTU/FT²SEC	
j	P_1	$\beta/2$	$-f_w$	v_∞	N_1	q	$Nu/\sqrt{R_e}$
1.0	1	0.25	0.0	5	.660	13.64	.530
				10	.446	81.1	.476
				20	.303	396.	.419
				30	.230	881.	.360
				40	.107	1380	.298
				50	.0364	2100.	.240
				60	.0118	2730	.185
1.0	1	0.25	0.25	5	.560	7.99	.312
				10	.446	44.9	.263
				20	.303	199.3	.217
				30	.230	423.	.172
				40	.107	652.	.129
				50	.0364	810.	.0925
				60	.0118	897.	.0640
				70	.00713	918.	.0432
1.0	1	0.25	0.5	5	.660	4.23	.165
				10	.446	21.3	.125
				20	.303	82.6	.0897
				30	.230	151.1	.0617
				40	.107	188.	.0371
				50	.0364	186.	.0213
				60	.0118	153.	.0109
				70	.00712	101.	.00477
1.0	1	0.25	1.0	5	.660	.74	.0287
				10	.446	1.71	.0101
				20	.303	2.07	2.25×10^{-3}
				30	.230	.87	3.56×10^{-4}
				40	.107	.117	2.31×10^{-5}
				50	.0364	.015	1.75×10^{-6}

TABLE I (Cont'd)

	ATM			KFT/SEC		BTU/FT^{2}SEC	
I	P_1	$\beta/2$	$-f_w$	v_∞	N_1	$\dot{q}$	$Nu/\sqrt{Re}$
1.0	1	0.5	0.5	5	.660	4.72	.184
				10	.446	24.1	.141
				20	.303	96.4	.105
				30	.230	182.	.0742
				40	.107	234.	.0463
				50	.0364	248.	.0283
				60	.0118	223.	.0160
				70	.00712	198.	.0093
1.0	10	0.25	0.0	5	.660	.0432x10^3	.533
				10	.445	.258x10^3	.472
				20	.301	[illegible]4x10^3	.417
				30	.230	2.85x10^3	.395
				40	.128	5.00x10^3	.305
				50	.0476	7.23x 10^3	.253
				60	.0194	9.55x10^3	.210
				70	.0121	12.47x10^3	.182
1.0	10	0.25	0.5	5	.660	13.4	.165
				10	.445	66.9	.122
				20	.301	260.	.0875
				30	.230	486.	.0615
				40	.128	621.	.0381
				50	.0476	630.	.0221
				60	.0194	538.	.0118
				70	.0121	373.	.00542

TABLE I (Concl'd)

	ATM			KFT/SEC		BTU/FT²SEC	
j	P_1	$\beta/2$	f_w	V_∞	N1	q	$Nu/\sqrt{R_e}$
0	1	0.5	0.0	20	.303	281.	.305
				30	.230	640.	.261
				40	.1071	1083.	.215
				50	.0364	1530.	.175
				60	.0118	1990	.142
0	1	0.5	0.5	30	.230	319.	.1305
				40	.1071	427.	.0975
				50	.0364	625.	.0711
				60	.0118	708.	.0505
0	1	0.5	0.5	30	.230	129.	.0525
				40	.1071	164.	.0328
				50	.0364	175.	.0201
				60	.0118	157.	.0112
0	1	0.5	1.0	30	.230	3.63	1.48×10^{-3}
				40	.1071	1.062	2.11×10^{-4}
				50	.0364	.213	2.44×10^{-5}

TABLE II

BOUNDARY LAYER PROFILES FOR EQUILIBRIUM AIR WITH ZERO BLOWING AT 1 ATM, $\beta/2=.25$, $j=1.0$

(a.) V_∞ =30,000 Ft/sec

η	Pr	f	f_η	g	T (°K)	Y (10^{-3}Ft)	N
0	.70	0.0	0.0	.00720	299.64	0	1.0
.21538	.56589	.012486	.12777	.096185	2944.4	.113	.46118
.42268	.66417	.055146	.28625	.20401	4417.0	.358	.38573
.63658	.56325	.13519	.46232	.33037	5794.7	.769	.32911
.84850	.62476	.25080	.62549	.46349	6457.0	1.303	.29950
1.0614	.72666	.39920	.76422	.61223	6947.5	1.953	.27586
1.2765	.82462	.57574	.87017	.76019	7428.6	2.726	.27370
1.4822	.87674	.76207	.93649	.87197	7752.3	3.556	.24301
1.6955	.89668	.96647	.97533	.94582	8180.0	4.536	.23425
1.9043	.88891	1.1720	.99186	.98012	8440.8	5.559	.23170
2.1296	.88381	1.3874	.99786	.99400	8554.7	6.650	.23068
2.3363	.88232	1.6020	.99954	.99846	8592.1	7.747	.23028
2.5428	.88192	1.8033	.99991	.99964	8602.1	8.801	.23018
2.7563	.88182	2.0348	.99999	.99993	8604.6	9.901	.23016
2.9647	.88180	2.2312	1.0	.99999	8605.0	10.96	.23015
3.1772	.88180	2.4436	1.0	1.0	8605.1	12.04	.23015

TABLE II (Cont'd)

(b) V_∞ = 40,000 Ft/sec

η	Pr	f	f_η	g	T	Y (10^{-3}Ft)	N
0	.7000	0	0	.004100	303.31	0	1.0
.19560	.57507	.0093789	.10650	.072651	3390.8	.108	.43158
.30606	.64345	.025369	.18425	.12420	4638.8	.234	.37525
.56034	.62122	.097781	.38789	.25630	6428.0	.724	.30302
.66688	.70484	.14377	.47532	.32557	6846.5	.988	.28279
.78005	.80581	.20277	.56709	.41199	7302.7	1.329	.26232
.87432	.87787	.25966	.63986	.49183	.77630	1.65	.24426
.97238	.87148	.32608	.71380	.57930	.88630	2.06	.22926
1.1358	1.0803	.45191	.82415	.72404	10918.	2.91	.18404
1.2616	1.2021	.56044	.89892	.84550	11974.	3.73	.14450
1.3650	1.2028	.65593	.94533	.92182	12448.	4.47	.12355
1.4573	1.2018	.74457	.97215	.96321	12645.	5.17	.11442
1.5447	1.2013	.83024	.98665	.98390	12735	5.86	.11022
1.6285	1.2011	.91319	.99390	.99334	12776.	6.50	.10836
1.7126	1.2010	.99700	.99741	.99748	12793.	7.18	.10755
1.7964	1.2010	1.0806	.99897	.99911	12800.	7.84	.10723
1.8800	1.2010	1.1641	.99962	.99971	12802.	8.51	.10712
1.9621	1.2010	1.2463	.99987	.99991	12803.	9.15	.10708
2.0442	1.2010	1.3284	.99996	.99998	12804.	9.81	.10706
2.1263	1.2010	1.4105	.99999	1.0	12804.	10.46	.10706
2.2029	1.2010	1.4870	1.0	1.0	12804.	11.08	.10706

NAD 1-1384

TABLE II (Cont'd)

(c) V_∞ =50, 000 Ft/sec

η	Pr	f	f_η	g	T	Y	N
					°K	(10^{-3}ft)	
0	.7000	0	0	2600×10^{-5}	300.56	0	1.0
.21737	.66450	.010886	.11195	.069254	4251.5	.138	.39523
.38933	.58504	.040377	.23423	.13994	6131.5	.410	.31533
.55379	.73863	.089330	.36242	.22712	7002.8	.784	.27360
.71244	.89394	.15698	.49134	.34477	8266.5	1.278	.23364
.85546	1.1139	.23583	.61341	.47837	1118.7	1.94	.17340
.92936	1.2030	.28386	.68843	.58408	12399.	2.39	.12512
.98945	1.1524	.32728	.75819	.68475	13326.	2.83	.086288
1.0374	1.0856	.36510	.81972	.76805	13783.	3.22	.069543
1.0804	1.0171	.40150	.87129	.83472	14149.	3.60	.058141
1.1081	.96811	.42602	.90052	.87092	14348.	3.83	.052802
1.1364	.92600	.45187	.92616	.90201	14518.	4.13	.048458
1.1653	.89105	.47897	.94753	.92782	14660.	4.42	.045016
1.2157	.84748	.52749	.97351	.95999	14836.	4.92	.040924
1.2626	.82275	.57345	.98719	.97825	14936.	5.42	.038698
1.3075	.80889	.61792	.99407	.98848	14992.	5.89	.037479
1.3513	.80091	.66159	.99738	.99409	15024.	6.36	.036924
1.3947	.79660	.70490	.99889	.99707	15041.	6.83	.036650
1.4378	.79438	.74803	.99956	.99860	15049.	7.28	.036509
1.4809	.79328	.79105	.99983	.99936	15054.	7.75	.036439
1.5239	.79275	.83402	.99994	.99973	15056.	8.22	.036406
1.5675	.79251	.87770	.99998	.99990	15057.	8.67	.036391
1.6112	.79241	.92136	1.0	.99997	15057.	0.15	.036384
1.6585	.79236	.96866	1.0	1.0	15057.	9.66	.036381

RAC 1-1384 R7-65

TABLE II (Concl'd)

(d) V_∞ =60,000 Ft/sec

η	Pr	f	f_η	g	T	Y (10^{-3} Ft)	N
0.0	.700	0.0	0.0	.00180	299.64	0	1.0
.065218	.65881	$.60014\times10^{-8}$	.020854	.015455	2243.8	.0169	.51689
.12402	.57071	.0025679	.046806	.029843	3269.7	.0529	.43763
.21494	.62517	.0088672	.093064	.057663	4762.3	.138	.36567
.28407	.56145	.016680	.13355	.080256	5730.5	.234	.33170
.37865	.62261	.032086	.19290	.11473	6439.4	.400	.30040
.42274	.67475	.041227	.22190	.13365	6707.2	.490	.28777
.51193	.79711	.063717	.28298	.17986	7263.9	.701	.26194
.59400	.90027	.089307	.34146	.23282	8080.4	.938	.23569
.63441	.86650	.10371	.37173	.26172	9013.2	1.081	.22635
.72438	1.1339	.14033	.44501	.34193	11365.0	1.482	.16548
.80167	1.2002	.17788	.53189	.46087	12960.0	1.940	.099357
.84595	1.060	.20295	.60410	.55552	13959.0	2.268	.063595
.89901	.82065	.23761	.71378	.68041	14945.0	2.731	.038446
.96468	.53333	.28968	.86361	.81960	16090.0	3.422	.022161
1.0612	.31225	.38006	.98338	.93899	17350.0	4.632	.014366
1.1065	.26520	.42502	.99607	.96714	17736.0	5.253	.013055
1.1817	.22498	.50007	.99983	.99300	18119.0	6.323	.012014
1.2180	.21647	.53638	1.0	1.0	18245.0	6.852	.011815

TABLE III

BOUNDARY LAYER PROFILES FOR EQUILIBRIUM AIR
WITH f_w = -0.5 AT P_1 = 1 ATM, $\beta/2$ = 0.25, j = 1.0
(a) V_∞ = 20,000 ft/sec

η	P_r	f	f_η	g	T	Y	N
					(°K)	(10^{-4} ft.)	
0	0.70000	-0.50000	0	0.01620	299.64	0.0	1.00000
0.21350	0.70000	-0.49621	0.038669	0.041396	749.23	0.383	0.67394
0.42206	0.69547	-0.48326	0.086914	0.073338	1263.5	1.125	0.62527
0.64083	0.70706	-0.45762	0.14982	0.11680	1902.0	2.34	0.53[illegible]7
0.84836	0.60196	-0.41928	0.22131	0.16585	2534.5	3.99	0.49311
1.0644	0.56323	-0.36252	0.30562	0.22081	2974.6	6.14	0.45897
1.2729	0.57328	-0.28963	0.39481	0.28144	3341.2	8.57	0.4[illegible]240
1.4811	0.57888	-0.19763	0.48981	0.35357	3496.7	11.37	0.39408
1.6949	0.56435	-0.082128	0.59062	0.44418	4324.6	14.71	0.39079
1.[illegible]	0.60728	0.051770	0.68942	0.54138	4883.3	18.68	0.35932
2.[illegible]	0.56388	0.21403	0.78487	0.63715	5373.2	23.57	0.33929
2.[illegible]	0.56168	0.38987	0.86186	0.72493	5738.7	28.88	0.33138
2.54[illegible]	0.56799	0.57528	0.91767	0.80181	5956.8	34.47	0.32203
2.7560	0.58311	0.77339	0.95605	0.86759	6115.6	40.47	0.31545
2.9676	0.59650	0.97834	0.97926	0.91861	6225.4	46.74	0.31072
3.1804	0.60517	1.1883	0.99149	0.95428	6296.5	53.24	0.30744
3.3915	0.61029	1.3982	0.99693	0.97634	6338.4	59.81	0.30544
3.6055	0.61313	1.6118	0.99905	0.98890	6361.7	66.54	0.30430
3.8189	0.61454	1.8251	0.99975	0.99523	6373.3	73.29	0.30373
4.0241	0.61517	2.0303	0.99994	0.99807	6378.4	79.80	0.30348
4.2450	0.61545	2.2511	0.99999	0.99935	6380.7	86.81	0.30337
4.4225	0.61554	2.4286	1.000	0.99976	6381.5	92.45	0.30333
4.6443	0.61558	2.6494	1.000	0.99996	6381.8	99.46	0.30331
4.7024	0.61559	2.7085	1.000	0.99998	6381.9	101.34	0.30331
4.7576	0.61559	2.7637	1.000	1.0000	6381.9	103.1	0.30331

TABLE III (Cont'd)

III(b) V_∞ = 30,000 ft/sec

η	P_r	f	f_η	g	T	Y	N
						(10^{-4} ft)	
0.0	0.70	-0.5000	0.0	0.00720	299.64	0.0	1.0
0.21288	0.69597	-0.49721	0.028334	0.025543	1015.5	0.411	0.68017
0.42434	0.70607	-0.48737	0.66672	0.050789	1869.0	1.31	0.54370
0.63573	0.58746	-0.46822	0.11632	0.81868	2699.4	2.81	0.47990
0.84459	0.56918	-0.43794	0.17514	0.11608	3227.3	4.74	0.44069
1.0642	0.61664	-0.39174	0.24777	0.16153	3718.9	7.23	0.40743
1.2744	0.64342	-0.33150	0.32748	0.22081	4639.0	10.21	0.37272
1.4822	0.46871	-0.25414	0.41854	0.28666	5304.2	14.05	0.33271
1.6967	0.56881	-0.15351	0.52027	0.36271	5993.3	18.81	0.32033
1.9031	0.61800	-0.035749	0.62059	0.44933	6041.7	24.10	0.30232
2.1203	0.69008	0.11029	0.72355	0.55676	6778.1	30.44	0.28430
2.3351	0.75817	0.27590	0.81607	0.67477	7134.7	37.62	0.26713
2.5452	0.84659	0.45548	0.88952	0.78913	7484.8	45.43	0.26339
2.7566	0.88245	0.64960	0.94338	0.88350	7806.2	54.21	0.24121
2.9663	0.89678	0.85115	0.97571	0.94623	8183.0	63.90	0.23421
3.1781	0.88832	1.0597	0.99138	0.97898	8431.7	74.28	0.23177
3.3915	0.88412	1.2721	0.99748	0.99306	8546.9	85.02	0.23076
3.6043	0.88243	1.4845	0.99940	0.99811	8589.1	95.84	0.23032
3.8168	0.88192	1.6970	0.99990	0.99963	8602.0	106.68	0.23018
4.0023	0.88180	1.8825	1.0	1.0	8605.1	116.15	0.23015

TABLE III (Cont'd)
III (c) V_∞ + 40,000 Ft/Sec

η	Pr	f	f_η	g	T	Y	N
						(10^{-4} FT)	
0	0.70000	-0.5000	0	0.00410	303.31	0.0	1.000
0.21266	0.69580	-0.49809	0.018653	0.018653	1100.9	.0392	0.66252
0.42154	0.70788	-0.49213	0.042020	0.030451	2010.1	1.[illegible]	0.53804
0.63728	0.57814	-0.47967	0.074745	0.049342	2805.3	2.56	0.47482
0.84406	0.57304	-0.46038	0.11303	0.070045	3334.5	4.27	0.43582
1.0616	0.66158	-0.43069	0.16145	0.098594	3980.1	6.48	0.40790
1.2765	0.60237	-0.39004	0.21899	0.13690	4916.4	9.33	0.36011
1.4837	0.56060	-0.33788	0.28603	0.17816	5700.0	12.89	0.33513
1.6941	0.59583	-0.26966	0.36434	0.22897	6219.9	17.18	0.31306
1.9060	0.66872	-0.18317	0.45403	0.29593	6679.3	22.25	0.29106
2.1200	0.77703	-0.075301	0.55556	0.38765	7174.2	28.31	0.26724
2.3348	0.89387	0.055631	0.66509	0.50848	7913.9	35.63	0.24021
2.5430	0.91793	0.20560	0.77445	0.64157	9816.7	45.01	0.21484
2.7578	1.1672	0.38352	0.88171	0.80539	11662	57.71	0.15531
2.9654	1.2023	0.57551	0.95987	0.93966	12537.	72.53	0.11946
3.1778	1.2012	0.78364	0.99355	0.99176	12769.	89.02	0.10867
3.2774	1.2010	0.88288	0.99876	0.99855	12798.	96.92	0.10734
3.3011	1.2010	0.90656	0.99950	0.99942	12801.	98.82	0.10717
3.3206	1.2010	0.92605	1.000	1.000	12804	100.4	0.10706

TABLE III (Cont'd)

III(d) $V_\infty = 50,000$ ft/sec

η	P_r	f	f_η	g	T	Y	N
						(10^{-3} ft)	
0	0.70000	-0.50000	0	0.002600	300.56	0.0	1.0000
0.20993	0.69651	-0.49888	0.011589	0.0087945	974.65	0.0306	0.68582
0.41873	0.70336	-0.49491	0.027198	0.017227	1778.7	0.0974	0.55551
0.63535	0.59312	-0.48680	0.048583	0.028280	2635.0	0.212	0.48584
0.84880	0.56732	-0.47374	0.074562	0.040388	3175.5	0.362	0.44515
1.0634	0.58590	-0.45447	0.10598	0.055713	3540.1	0.548	0.40284
1.2706	0.66160	-0.42884	0.14242	0.076094	4516.2	0.768	0.38069
1.4863	0.56180	-0.39323	0.18912	0.10149	5402.9	1.071	0.34658
1.6981	0.56885	-0.34749	0.24421	0.13067	5994.6	1.436	0.32081
1.9031	0.62498	-0.29120	0.30661	0.16703	6458.8	1.849	0.29991
2.1222	0.72734	-0.21566	0.38514	0.22079	6950.6	2.369	0.27617
2.3352	0.85728	-0.12431	0.47407	0.29592	7568.7	2.977	0.25413
2.5463	0.88729	-0.013569	0.57730	0.39792	9522.1	3.779	0.21964
2.7579	1.2039	0.12118	0.70401	0.56402	12217.0	4.932	0.13327
2.9657	1.0288	0.28499	0.87841	0.82615	14102.0	6.553	0.059453
3.1780	0.82367	0.48470	0.98744	0.97757	14933.0	8.662	0.038779
3.2275	0.80843	0.53473	0.99436	0.98883	14994.0	9.186	0.037438
3.3146	0.79509	0.62159	0.99921	0.99811	15047.0	10.12	0.036554
3.3401	0.79328	0.64712	0.99975	0.99937	15054.0	10.39	0.036439
3.3576	0.79236	0.66460	1.0000	1.0000	15057.0	10.58	0.03681

TABLE III (Cont'd)
III (e) V_∞ = 60,000 Ft/Sec

η	P_r	f	f_η	g	T	Y	N
						10^{-3} FT	
0	0.70000	-0.50000	0	0.001801	299.81	0.0	1.0000
0.22075	0.69967	-0.49924	0.0069958	0.0050482	816.56	0.0252	0.68424
0.42528	0.69523	-0.015444	0.0090099	1383.4	0.0729	0.60674	
0.63035	0.68868	-0.49280	0.02692	0.014239	2101.5	0.148	0.52801
0.85191	0.58596	-0.48542	0.04081[illegible]	0.020684	2716.4	0.262	0.47870
1.0678	0.56685	-0.47482	0.057828	0.027789	3162.5	0.401	0.44547
1.2702	0.620[illegible]9	-0.46126	0.076633	0.035978	3740.7	0.555	0.43326
1.4815	0.6[illegible]58	-0.44268	0.099831	0.047343	4208.1	0.744	0.39677
1.6959	[illegible].59276	-0.41834	0.12826	0.062183	4981.4	0.988	0.35480
1.9018	0.55977	-0.33863	0.16120	0.078131	5670.3	1.278	0.33411
2.1204	0.58938	-0.34900	0.20248	0.098936	6167.1	1.639	0.31338
2.3331	0.65250	-0.30103	0.25009	0.12593	6604.2	2.046	0.29271
2.5453	0.75528	-0.24213	0.30663	0.16399	7077.1	2.524	0.26977
2.7556	0.87835	-0.17092	0.37266	0.21881	7767.4	3.090	0.24251
2.9674	0.96767	-0.083651	0.45346	0.29719	10197.	3.875	0.20388
3.1777	1.1959	0.022967	0.57328	0.46795	13028.	5.036	0.096349
3.3911	0.51044	0.17211	0.85807	0.83136	16207.	[illegible].980	0.021255
3.5578	0.21647	0.33072	1.0000	1.0000	18245.	9.201	0.011819

TABLE III (Concl'd)
III (f_s) V_∞ = 70,000 ft/sec.

η	P_t	f	f_s	g	T	Y	N
						10^{-3} ft	
0	0.70000	-0.50000	0	0.0013220	299.54	0	1.0000
0.20679	0.700000	-0.49971	0.0030595	0.0025198	263.85	0.016	0.73108
0.42350	0.69749	-0.49858	0.0073931	0.0042525	925.66	0.047	0.6?446
0.63046	0.69541	-0.49658	0.012147	0.0061758	1296.3	0.091	0.61956
0.85606	0.70348	-0.49315	0.018501	0.0088357	1782.8	0.157	0.55396
1.?604	0.64538	-0.48868	0.025435	0.011824	2307.7	0.237	0.51167
1.2748	0.58477	-0.48199	0.034354	0.015386	2729.9	0.346	0.47741
1.4803	0.56244	-0.47442	0.043303	0.018887	3039.9	0.456	0.45411
1.6970	0.57433	-0.46384	0.054680	0.023484	3370.2	0.595	0.43015
1.9032	0.57892	-0.45130	0.067158	0.028948	3487.7	0.746	0.39418
2.1274	0.66428	-0.43452	0.082911	0.036848	4361.2	0.936	0.38875
2.3349	0.59232	-0.41577	0.10027	0.045915	4984.3	1.153	0.35450
2.5403	0.55776	-0.39296	0.12046	0.055902	5598.6	1.410	0.33655
2.7580	0.57465	-0.36411	0.14518	0.068719	6046.4	1.723	0.31818
2.9640	0.62151	-0.33148	0.17229	0.084134	6430.4	2.061	0.30081
3.1780	0.70252	-0.29119	0.20510	0.10507	68?5.8	2.463	0.28138
3.3952	0.81789	-0.24250	0.24434	0.13812	73?6.6	2.943	0.25877
3.6029	0.88296	-0.18737	0.28828	0.18347	8576.0	3.509	0.23041
3.8153	1.1519	-0.12054	0.34400	0.25795	11526.0	4.339	0.15921
4.0262	0.82623	-0.037821	0.46616	0.49882	14922.0	5.666	0.038933
4.2431	0.p7715	0.11208	0.93935	0.?88695	23142.0	8.505	0.0093190
4.2794	0.24822	0.14708	0.98613	0.96208	2462.0	9.181	0.0078703
4.2938	0.27089	0.16142	1.0000	1.0000	25177.0	9.467	0.0071298

TABLE IV

BOUNDARY LAYER PROFILES FOR EQUILIBRIUM AIR WITH
f_w = -1.0 at P_i = 1 ATM, $\beta/2$ = 0.25, j = 1.0
(a) V_∞ = 20,000 ft/sec

η	Pr	f	f_η	g	T	Y	N
					(°K)	(10^{-3}Ft)	
0	0.70000	-1.0000	0	0.01620	299.64	0	1.0000
0.22134	0.70000	-0.99948	0.0047427	0.016950	313.40	0.0240	0.97556
0.42171	0.70000	-0.99807	0.0093548	0.017774	328.48	0.0467	0.95086
0.63158	0.70000	-0.99557	0.014579	0.018807	347.32	0.0718	0.92274
0.84929	0.70000	-0.93176	0.020516	0.020107	370.99	0.0996	0.89128
1.0578	0.70000	-0.98684	0.026858	0.021642	399.61	0.128	0.84145
1.2711	0.70000	-0.98034	0.034141	0.023587	434.24	0.160	0.82380
1.4915	0.70000	-0.97191	0.032465	0.026063	478.60	0.195	0.79456
1.6903	0.70000	-0.96260	0.051269	0.029852	526.64	0.230	0.75757
1.9015	0.70000	-0.95066	0.062112	0.032621	596.00	0.272	0.70794
2.1239	0.70000	-0.93538	0.075701	0.037749	686.39	0.322	0.68389
2.3521	0.70000	-0.91629	0.091931	0.044424	799.46	0.383	0.68377
2.5492	0.69768	-0.89666	0.10759	0.051397	916.13	0.443	0.68458
2.7563	0.69588	-0.87251	0.12593	0.060223	1059.9	0.515	0.66795
2.9645	0.69553	-0.84413	0.14736	0.071440	1234.6	0.600	0.63067
3.1705	0.69509	-0.81126	0.17240	0.085708	1454.3	0.697	0.59691
3.3923	0.70257	-0.76958	0.20440	0.10577	1752.4	0.822	0.55782
3.6081	0.67863	-0.72156	0.24166	0.13169	2149.4	0.970	0.52425
3.8123	0.60877	-0.66812	0.28274	0.16051	2482.1	1.137	0.49739
4.0294	0.57912	-0.60141	0.33309	0.19594	2794.1	1.341	0.47250
4.2436	0.56393	-0.52412	0.38989	0.23713	3081.5	1.570	0.45117
4.4275	0.57286	-0.44744	0.44459	0.27929	3329.5	1.789	0.43326
4.6452	0.59749	-0.34299	0.51615	0.33978	3607.5	2.078	0.41465
4.8518	0.66479	-0.22865	0.59110	0.41128	4106.8	2.384	0.40102
5.8116	0.56714	0.50767	0.91587	0.79264	5933.4	4.544	0.32310
6.8951	0.61306	1.5653	0.99895	0.98855	6361.1	7.810	0.30433
7.5364	0.61559	2.2064	1.0000	1.0000	6381.9	9.843	0.30331

TABLE IV (Cont'd)

(b) V_∞ = 30,000 ft/sec

η	P_r	f	f_η	g	T	Y	N
0	0.70000	-1.0000	0	0.007200	299.64	0	1.0000
0.21510	0.70000	-0.99977	.0021116	0.0073151	304.38	0.0196	0.99136
0.42818	0.70000	-0.99910	.0042679	0.0074516	310.00	0.394	0.98142
0.63899	0.70000	-0.99796	0.0064757	0.0076104	316.53	0.0593	0.97026
0.84724	0.70000	-0.99638	0.0087429	0.0077950	324.12	0.0795	0.95779
1.0696	0.70000	-0.99416	0.011276	0.0080291	333.72	0.102	0.94274
1.27[illegible]6	0.70000	-0.99164	0.013697	0.0082817	344.07	0.122	0.92739
1.4865	0.70000	-0.98840	0.016423	0.0086017	357.16	0.145	0.90916
1.6970	0.70000	-0.98465	0.019273	0.0089779	372.53	0.168	0.88937
1.9027	0.70000	-0.98038	0.022267	0.0094199	390.56	0.192	0.86819
2.1296	0.70000	-0.97492	0.025926	0.010026	415.67	0.220	0.83404
2.3379	0.70000	-0.96914	0.029576	0.010703	442.78	0.248	0.81862
2.5416	0.70000	-0.96273	0.033493	0.011505	475.05	0.276	0.79707
2.7529	0.70000	-0.95519	0.038040	0.012530	516.35	0.307	0.76681
2.9682	0.70000	-0.94641	0.043364	0.013848	569.34	0.341	0.72717
3.1723	0.70000	-0.93699	0.049271	0.015443	632.98	0.378	0.69656
3.3948	0.70000	-0.92522	0.056720	0.017637	719.05	0.424	0.67784
3.6028	0.69970	-0.91262	0.064627	0.020177	814.82	0.473	0.68400
3.8122	0.69739	-0.89817	0.073457	0.023258	930.30	0.528	0.68459
4.0204	0.69587	-0.88188	0.083256	0.026978	1066.0	0.591	0.66629
4.2423	0.69551	-0.86209	0.095428	0.032047	1243.0	0.668	0.62905
4.4410	0.69511	-0.84189	0.10827	0.037905	1445.6	0.748	0.59806
4.6501	0.70141	-0.81764	0.12418	0.045885	1713.7	0.847	0.56268
4.8559	0.69347	-0.79021	0.14285	0.056340	2078.9	0.964	0.52951
5.0872	[illegible]	-0.75438	0.16779	0.070692	2465.4	1.122	0.49877
6.8227	0.59758	-0.16881	0.59667	0.40156	6193.3	3.619	0.31214
7.8209	0.88195	[illegible].51809	0.94472	0.88254	7801.4	7.024	0.24136
8.5719	0.88180	[illegible].3570	1.0000	1.0000	8605.1	10.701	0.23015

TABLE IV (Cont'd)

(c) V_∞ = 40,000 ft/sec

η	Pr	f	f_η	g	T	Y	N
						10^{-3}ft	
0	0.70000	-1.0000	0	0.004100	303.31	0	1.0000
0.21993	0.70000	-0.99988	0.0010955	0.0041076	303.69	0.0173	0.99932
0.41972	0.70000	-0.9956	0.0020934	0.0041158	304.09	0.030	0.99858
0.83874	0.70000	-0.99824	0.0041965	0.0041373	305.15	0.662	0.99667
1.2767	0.70000	-0.99592	0.0064138	0.0041676	306.65	0.101	0.99399
1.6935	0.70000	-0.99280	0.0085484	0.0042067	308.57	0.134	0.99056
2.1481	0.70000	-0.98838	0.010914	0.0042649	311.44	0.171	0.98554
2.7563	0.70000	-0.98076	0.14166	0.0043792	317.06	0.220	0.97592
3.3957	0.70000	-0.97057	0.17749	0.0045681	326.35	0.274	0.96067
4.0978	0.70000	-0.95664	0.02200	0.0049094	343.09	0.334	0.93507
4.6867	0.70000	-0.94254	0.025983	0.0053768	365.97	0.389	0.90368
5.0960	0.70000	-0.93127	0.029102	0.0058581	389.49	0.429	0.87527
5.6841	0.70000	-0.91264	0.034436	0.0069312	441.81	0.493	0.82475
6.0878	0.70000	-0.89787	0.038858	0.0080517	495.84	0.541	0.78735
6.6467	0.70000	-0.87168	0.047777	0.010848	630.26	0.628	0.70196
7.0956	0.70000	-0.85108	0.055829	0.013866	770.15	0.702	0.69001
7.6997	0.69583	-0.81284	0.71503	0.020938	1084.5	0 846	0.66634
8.0948	0.69520	-0.78189	0.85746	0.28502	1401.0	0.472	0.60817
8.6906	0.66023	-0.72218	0.11720	0.049021	2237.0	1.245	0.52093
9.0971	0.57653	-0.66845	0.14874	0.070569	2823.5	1.514	0.47342
9.6929	0.59327	-0.56102	0.21727	0.12141	3583.0	2.039	0.41289
10.095	0.61713	-0.46028	0.28768	0.18580	4816.7	2.530	0.36518
10.695	0.61418	-0.24247	0.45172	0.33329	6370.3	3.670	0.30593
11.092	0.81008	-0.032447	0.61407	0.51115	7321.8	4.756	0.26168
11.560	1.1752	0.31465	0.89026	0.86258	11734.	6.921	0.15279
11.690	1.2010	0.43720	0.99988	1.000	12804.	7.871	0.10706

TABLE IV (Concl'd)

(d) V_∞ = 50,000 ft/sec

η	Pr	f	f_η	g	T	Y	N
						10^{-3}ft	
0	0.70000	-1.0000	0	0.002600	300.56	0	1.0000
0.25198	0.70000	-0.99990	0.00083107	0.0026007	300.65	0.0178	0.99964
0.78377	0.70000	-0.99899	0.0025871	0.0026026	300.91	0.0555	0.99936
1.3432	0.70000	-0.99702	0.0044389	0.0026055	301.30	0.0952	0.99863
1.9860	0.70000	-0.99348	0.0065747	0.0026107	302.00	0.141	0.99735
3.0175	0.70000	-0.98492	0.010035	0.0026256	304.04	0.214	0.99365
3.9054	0.70000	-0.97467	0.013071	0.0026510	307.46	0.278	0.98755
4.6763	0.70000	-0.96355	0.015790	0.0026901	312.74	0.334	0.97835
5.4649	0.70000	-0.94996	0.018711	0.0027594	322.09	0.394	0.96270
6.2896	0.70000	-0.93318	0.022035	0.0028891	339.56	0.458	0.93555
7.7829	0.70000	-0.89496	0.029670	0.0034827	419.56	0.590	0.83343
9.0783	0.70000	-0.85005	0.40992	0.0051749	643.30	0.744	0.69511
10.218	0.69560	-0.79327	0.060572	0.0097278	1201.2	0.982	0.63878
11.169	0.61920	-0.72202	0.093117	0.020953	2432.4	1.368	0.50236
11.937	0.61777	-0.63291	0.14413	0.041097	3725.4	1.933	0.43070
12.581	0.57079	-0.51715	0.22449	0.081886	5274.4	2.698	0.33045
13.107	0.66828	-0.36975	0.34619	0.14769	6677.2	3.734	0.28969
13.558	0.88854	-0.17795	0.51855	0.27649	7863.6	4.997	0.24009
13.897	1.1921	0.28702	0.71387	0.48422	11885.	6.594	0.14679
14.070	1.0845	0.16517	0.87109	0.71698	13791.	7.849	0.069281
14.163	0.90237	0.25072	0.96582	0.86533	14614	8.713	0.046115
14.233	0.82210	0.32008	1.0000	0.95325	14939.	9.433	0.03864
14.276	0.79675	0.36312	1.0000	0.99237	15040.	9.891	0.036659
14.287	0.79236	0.37333	1.000	1.0000	15057.	10.000	0.036381

TABLE V

BOUNDARY LAYER PROFILES FOR EQUILIBRIUM AIR

WITH ZERO BLOWING AT P_1 = 1 ATM. B/ℓ = .5 , j=O

(a) V_∞ = 20,000 Ft/sec

η	Pr	f	f_η	g	T	Y	N
					(°K)	(ft)	
0	0.70000	0	0	0.01620	299.64	0	1.00
0.021734	0.70000	1.157×10^{-4}	0.01182	0.023405	430.97	3.9756×10^{-6}	0.82571
0.098305	0.69624	2.8356×10^{-3}	0.061165	0.055796	988.24	2.1217×10^{-5}	0.68472
0.21437	0.70564	0.014807	0.14779	0.11321	1854.7	1.1344×10^{-4}	0.54538
0.42134	0.551[illegible]	0.063352	0.32257	0.22335	2991.8	3.7744×10^{-4}	0.45772
0.64006	0.5893[illegible]	0.15378	0.50150	0.34570	3560.3	7.6678×10^{-4}	0.40591
0.84920	0.6562[illegible]	0.27503	0.65359	0.48178	4552.6	1.2451×10^{-3}	0.37786
1.0685	0.55713	0.43346	0.78537	0.61506	5576.0	1.8830×10^{-3}	0.34564
1.2796	0.56151	0.60943	0.87587	0.72296	5732.5	2.6327×10^{-3}	0.33162
1.4031	0.56845	0.79385	0.93274	0.81092	5980.2	3.4095×10^{-3}	0.32095
1.6962	0.58731	0.99685	0.96847	0.88309	6150.1	4.2764×10^{-3}	0.31401
1.9167	0.60066	1.2127	0.98754	0.93546	6259.5	5.2314×10^{-3}	0.30916
2.1271	0.60805	1.4215	0.99554	0.96660	6320.1	6.1325×10^{-3}	0.30632
2.3397	0.61210	1.6335	0.99863	0.98431	6353.2	7.0755×10^{-3}	0.30472
2.5806	0.61427	1.8743	0.99970	0.99401	6371.0	8.1534×10^{-3}	0.30384
2.8102	0.61512	2.1038	0.99994	0.99784	6378.0	9.1844×10^{-3}	0.30350
2.9668	0.61537	2.2604	0.99998	0.99899	6330.1	9.8886×10^{-3}	0.30340
3.1816	0.61552	2.4751	1.0	0.99967	6381.3	1.0855×10^{-2}	0.30334
3.392[illegible]	0.61557	2.6863	1.0	0.99990	6381.7	1.1805×10^{-2}	0.30332
3.5674	0.61558	2.8610	1.0	0.99997	6361.8	1.2592×10^{-2}	0.30331
3.6911	0.61559	2.984[illegible]	1.0	0.99999	6381.9	1.3149×10^{-2}	0.30331
3.8003	0.61559	3.0939	1.0	0.99999	6381.9	1.3641×10^{-2}	0.30331
3.9605	0.61559	3.2540	1.0	1.0	6381.9	1.4362×10^{-2}	0.30331

TABLE V (Cont'd)

(b) V_∞ =30, 000 Ft/sec

η	Pr	f	f_η	g	T	Y	N
0	0.7000	0.0	0.0	7.2×10^{-3}	299.64	0.0	1.0
0.023376	0.7000	1.1854×10^{-4}	0.011108	0.014461	594.45	4.385×10^{-6}	0.70904
0.095598	0.69901	2.4612×10^{-3}	0.055270	0.043381	1633.7	3.8693×10^{-5}	0.57298
0.21480	0.56278	0.014341	0.14663	0.098479	2979.8	1.6271×10^{-4}	0.45859
0.42450	0.66006	0.063634	0.32498	0.21215	4526.6	5.2139×10^{-4}	0.37942
0.66955	0.56848	0.16945	0.53522	0.36062	5981.4	1.2216×10^{-3}	0.32089
0.84257	0.62764	0.27350	0.66408	0.47407	6497.0	1.8586×10^{-3}	0.29741
1.0620	0.73897	0.43440	0.79658	0.63141	7004.3	2.8232×10^{-3}	0.27307
1.2783	0.84195	0.61767	0.89110	0.77930	7464.0	3.9374×10^{-3}	0.26667
1.4821	0.88383	0.80558	0.94855	0.88616	7819.2	5.1295×10^{-3}	0.24084
1.6941	0.89503	1.0105	0.98067	0.95334	8234.3	6.5259×10^{-3}	0.23359
1.9152	0.88681	1.2291	0.99430	0.98449	8476.2	8.0705×10^{-3}	0.23145
2.1222	0.88339	1.4354	0.99848	0.99525	8565.2	9.5495×10^{-3}	0.23057
2.3318	0.58221	1.6449	0.99967	0.99877	8594.8	0.011059	0.23026
2.5800	0.88186	1.8930	0.99996	0.99980	8603.4	0.012851	0.23017
2.8120	0.88181	2.1250	1.0	0.99997	8604.9	0.014527	0.23015
2.9666	0.88180	2.2797	1.0	0.99999	8605.1	0.015644	0.23015
3.1825	0.88180	2.4955	1.0	1.0	9605.1	0.017203	0.23015

TABLE V (Cont'd)

(c) V_∞ = 40,000 Ft/sec

η	Pr	f	f_η	g	T	Y	N
0	0.7000	0.0	0.0	4.1×10^{-3}	303.31	0.0	1.0
0.025438	0.7000	1.2196×10^{-4}	0.010627	0.010966	789.89	5.0077×10^{-6}	0.68893
0.092423	0.65826	2.0064×10^{-3}	0.047633	0.034828	2246.4	4.2008×10^{-5}	0.52018
0.21046	0.62288	0.012380	0.13036	0.080563	3755.1	1.7681×10^{-4}	0.43907
0.36899	0.56353	0.042916	0.25755	0.15915	5378.1	4.8146×10^{-4}	0.34206
0.4900	0.58892	0.080345	0.36093	0.[illegible]2229	6163.3	8.1875×10^{-4}	0.31556
0.64330	0.69681	0.1456	0.48995	0.3[illegible]	6809.3	1.3494×10^{-3}	0.28466
0.72302	0.76655	0.18728	[illegible]55521	0.37874	7127.4	1.6760×10^{-3}	0.26925
0.85288	0.87524	0.26599	0.65599	0.48868	7738.1	2.2878×10^{-3}	0.24520
0.96209	0.86641	0.34213	0.73707	0.58740	8989.8	2.9360×10^{-3}	0.22815
1.0692	0.99390	0.42501	0.80884	0.68121	10365.	3.7060×10^{-3}	0.20019
1.1463	1.1228	0.48924	0.85715	0.75723	11266	4.3548×10^{-3}	0.17076
1.2936	1.2036	0.62149	0.93367	0.89133	12279	5.7770×10^{-3}	0.13119
1.4166	1.2019	0.73891	0.97248	0.95816	12622	7.0823×10^{-3}	0.11548
1.4836	1.2015	0.80457	0.98435	0.97743	12707	7.8209×10^{-3}	0.11152
1.5908	1.2011	0.91063	0.99430	0.99255	12772	9.0198×10^{-3}	0.10851
1.6961	1.2010	1.0156	0.99812	0.99781	12794	0.010209	0.10749
1.8008	1.2010	1.1202	0.99944	0.99943	12801	0.011394	0.10717
1.9173	1.2010	1.2367	0.99987	0.99989	12803	0.012715	0.10708
2.0424	1.2010	1.3617	0.99998	0.99998	12804	0.014132	0.10706
2.1109	1.2010	1.4303	0.99999	1.0	12804	0.014909	0.10706
2.200	1.2010	1.5193	1.0	1.0	12804	0.015919	0.10706

TABLE V (Cont'd)

(d) V_∞ =50,000 Ft/sec

η	Pr	f	f_η	g	T	Y	N
0.0	0.7000	0.0	0.0	2.60×10^{-3}	300.56	0.0	1.0
0.030394	0.6959	1.5813×10^{-4}	0.011666	9.5562×10^{-3}	1051.8	6.7764×10^{-6}	0.67120
0.096096	0.58793	2.0049×10^{-3}	0.046484	0.029371	2694.0	4.9041×10^{-5}	0.48114
0.21620	0.66434	0.012236	0.12606	0.071261	4332.3	1.9762×10^{-4}	0.39104
0.42391	0.61776	0.055167	0.29069	0.16159	6399.7	6.9319×10^{-4}	0.30293
0.64482	0.86486	0.13984	0.47598	0.30383	[illegible]640.2	1.5155×10^{-3}	0.24881
0.84864	1.1441	0.25480	0.65493	0.49948	[illegible]1457.	2.7978×10^{-3}	0.16214
1.0386	1.0454	0.39898	0.86983	0.81388	[illegible]4035.	4.7861×10^{-3}	0.061359
1.06[illegible]	0.98515	0.42664	0.90217	0.85834	14279.	5.1899×10^{-3}	0.054623
1.10[illegible]	0.92707	0.46062	0.93398	0.90122	14514.	5.6898×10^{-3}	0.048565
1.1500	0.87678	0.50154	0.96133	0.93836	14718.	6.2965×10^{-3}	0.043652
1.2151	0.83037	0.56503	0.98510	0.97262	14905.	7.2461×10^{-3}	0.039377
1.2545	0.81479	0.60399	0.99226	0.98413	14968.	7.8328×10^{-3}	0.037995
1.2779	0.80857	0.62722	0.99488	0.98872	14994.	8.1836×10^{-3}	0.037450
1.3114	0.80214	0.66057	0.99726	0.99324	15019.	8.6883×10^{-3}	0.037003
1.3504	0.79758	0.69955	0.99874	0.99639	15037.	9.2791×10^{-3}	0.036712
1.3885	0.79510	0.73761	0.99943	0.99811	15046.	9.8565×10^{-3}	0.036555
1.4206	0.79391	0.76973	0.99972	0.99893	15051.	0.010344	0.036479
1.4600	0.79310	0.80909	0.99989	0.99949	15054.	0.010942	0.036428
1.4950	0.79273	0.84404	0.99995	0.99974	15056.	0.011473	0.036405
1.5328	0.79252	0.88190	0.99998	0.99989	15057.	0.012048	0.036392
1.5867	0.79240	0.93575	1.0	0.99997	15057.	0.012867	0.036384
1.6078	0.79238	0.95685	1.0	0.99999	15057.	0.013188	0.036382
1.6347	0.79236	0.98377	1.0	1.0	15057.	0.013597	0.036381

TABLE V (Concl'd)

(e) V_∞ =60,000 Ft/sec

η	Pr	f	f_η	g	T	Y	N
0	0.7000	0	0	1.8010×10^{-3}	299.81	0	1.0
0.22648	0.58653	0.011470	0.11459	0.063691	5049.6	2.2049×10^{-4}	0.35204
0.42200	0.68965	0.046950	0.25109	0.13905	6776.2	7.0735×10^{-4}	0.28448
0.63313	0.88316	0.11484	0.41363	0.27429	9451.7	1.5788×10^{-3}	0.22044
0.85122	0.93076	0.23184	0.68804	0.62417	14499.0	3.4636×10^{-3}	0.048870
0.90844	0.66099	0.27473	0.81252	0.75772	15570.0	4.2468×10^{-3}	0.028586
0.95276	0.49151	0.31277	0.90093	0.84179	16304.0	4.9493×10^{-3}	0.020517
0.98188	0.41160	0.33966	0.94356	0.88380	16711.0	5.4495×10^{-3}	0.017568
1.0124	0.34830	0.36896	0.97267	0.91755	17055.0	6.0003×10^{-3}	0.015433
1.0354	0.31554	0.39146	0.98550	0.93712	17323.0	6.4294×10^{-3}	0.014466
1.0615	0.28637	0.41733	0.99354	0.95455	17563.0	6.9304×10^{-3}	0.013639
1.0821	0.26827	0.43782	0.99679	0.96536	17711.0	7.3329×10^{-3}	0.013142
1.1061	0.25143	0.46181	0.99868	0.97542	17849.0	7.8097×10^{-3}	0.012690
1.1254	0.24063	0.48110	0.99939	0.98187	17937.0	8.1970×10^{-3}	0.012406
1.1483	0.23107	0.50395	0.99977	0.98301	18029.0	8.6506×10^{-3}	0.012161
1.1669	0.22616	0.52257	0.99991	0.99204	18101.0	9.0392×10^{-3}	0.012045
1.1893	0.22139	0.54490	0.99997	0.99596	18172.0	9.4970×10^{-3}	0.011933
1.1989	0.21966	0.55454	0.99999	0.99738	18198.0	9.6955×10^{-3}	0.011893
1.2098	0.21790	0.56544	0.99999	0.99883	18224.0	9.9202×10^{-3}	0.011852
1.2197	0.21647	0.57535	1.0	1.0	18245.0	1.0125×10^{-2}	0.011819

TABLE VI

BOUNDARY LAYER PROFILES FOR EQUILIBRIUM AIR WITH

$f_w = -0.5$ at $P_1 = 1$ atm, $\beta/2 = 0.5$, $j = 0$

(a) $V_\infty = 30,000$ ft/sec

η	Pr	f	f_η	g	T	Y	N
					°K	(ft)	
0	0.7000	0.5000	0	7.2×10^{-3}	299.64	0	1.0
0.21094	0.69569	0.49574	0.043584	0.029405	1153.9	6.3561×10^{-5}	0.64979
0.4247	0.65374	0.47971	0.10615	0.06270	2267.9	2.2079×10^{-4}	0.51497
0.63814	0.56205	0.45007	0.17977	0.099018	2988.0	2.6010×10^{-4}	0.45799
0.83455	0.58120	0.40721	0.25800	0.13957	3512.8	7.4763×10^{-4}	0.41919
1.0857	0.66148	0.32875	0.36850	0.21141	4517.0	1.2169×10^{-3}	0.38000
1.2698	0.55639	0.25280	0.45754	0.27464	5549.7	1.6799×10^{-3}	0.36103
1.4679	0.56638	0.15254	0.55455	0.34787	5906.3	2.2845×10^{-3}	0.32432
1.7796	0.64114	0.043295	0.7000	0.48900	6551.6	3.4298×10^{-3}	0.29500
1.9410	0.70307	0.16190	0.76899	0.57610	6838.3	4.1224×10^{-3}	0.28131
2.1162	0.76929	0.30275	0.83697	0.67747	7139.7	4.9606×10^{-3}	0.26671
2.3322	0.85021	0.49130	0.90545	0.79666	7501.9	6.0998×10^{-3}	0.26102
2.5583	0.88930	0.70212	0.95557	0.89618	7870.8	7.4484×10^{-3}	0.23951
2.7959	0.89356	0.93304	0.98403	0.95919	8277.7	9.0294×10^{-3}	0.23313
2.9780	0.88736	1.1132	0.99375	0.98249	8460.0	0.010302	0.23156
3.1186	0.88462	1.2532	0.99723	0.99157	8534.5	0.011303	0.23090
3.3068	0.88275	1.4410	0.99918	0.99715	8581.2	0.012654	0.23040
3.5168	0.88204	1.6510	0.99982	0.99927	8599.0	0.014169	0.23021
3.7488	0.88184	1.8830	0.99998	0.99987	8604.0	0.015844	0.23016
3.9072	0.88181	2.0413	0.99999	0.99996	8604.8	0.016988	0.23015
4.2570	0.88180	2.3912	1.0	1.0	8605.1	0.019515	0.23015

TABLE VI (Cont'd)

(b) V_∞ = 40,000 ft/sec

η	Pr	f	f_η	g	T	Y	N
0	0.7000	-0.5000	0	4.10×10^{-3}	303.31	0	1.0
0.21948	0.69542	-0.49694	0.030147	0.018765	1290.0	6.2630×10^{-5}	0.62591
0.42017	0.62646	-0.48717	0.069038	0.038114	2397.8	1.9875×10^{-4}	0.50778
0.63702	0.56598	-0.46669	0.1214[illegible]	0.061564	3138.3	4.2650×10^{-4}	0.45009
0.84100	0.57778	-0.43620	0.17906	0.089358	3466.0	7.0275×10^{-4}	0.39123
1.0716	0.51294	-0.38649	0.25422	0.13356	4845.0	1.1155×10^{-3}	0.36370
1.3268	0.56482	-0.30945	0.35123	0.19066	5850.7	1.7491×10^{-3}	0.32896
1.4907	0.60237	-0.24642	0.41857	0.23564	6273.6	2.2395×10^{-3}	0.31060
1.6951	0.68330	-0.15181	0.50802	0.30763	6746.7	2.9494×10^{-3}	0.28777
1.9242	0.81347	-0.023232	0.61604	0.41832	7336.9	3.9093×10^{-3}	0.26118
2.1157	0.89473	0.10366	0.71148	0.53694	8243.3	4.8907×10^{-3}	0.23507
2.3709	1.0564	0.30167	0.83893	0.71200	10765.0	6.6874×10^{-3}	0.18843
2.5597	1.2045	0.46840	0.92326	0.86317	12099.0	8.4342×10^{-3}	0.13920
2.7089	1.2022	0.60979	0.96808	0.94666	12570.0	9.9904×10^{-3}	0.11793
2.8427	1.2014	0.74089	0.98844	0.98234	12729.0	0.011462	0.11053
2.9712	1.2011	0.86845	0.99637	0.99504	12783.0	0.012904	0.10803
3.0979	1.2010	0.99492	0.99901	0.99882	12799.0	0.014337	0.10729
3.2242	1.2010	1.1211	0.99977	0.99976	12803.0	0.015768	0.10711
3.3503	1.2010	1.2472	0.99995	0.99996	12804.0	0.017197	0.10707
3.4764	1.2010	1.3733	0.99999	0.99999	12804.0	0.018627	0.10706
3.6026	1.2010	1.4995	1.0	1.0	12804.0	0.020056	0.10706

TABLE VI (Cont'd)

(c) V_∞ = 50,000 ft/sec

η	Pr	f	f_η	g	T	Y	N
0	0.7000	-0.5000	0	2.600×10^{-3}	300.56	0	1.0
0.02052	0.69565	-0.49814	0.19635	0.010809	1175.1	4.8813×10^{-5}	0.64506
0.076269	0.57642	-0.46401	0.11149	0.047627	3428.4	5.1615×10^{-4}	0.42652
0.094697	0.66473	-0.43973	0.15281	0.065928	4110.2	7.6480×10^{-4}	0.40157
1.40[illegible]7	0.56843	-0.34236	0.28212	0.12970	5979.6	1.7185×10^{-3}	0.32151
1.9077	0.80070	-0.15375	0.47290	0.26092	7279.9	3.3795×10^{-3}	0.26180
2.304[illegible]	1.1086	0.071464	0.67228	0.47453	11139.0	5.6015×10^{-3}	0.17482
2.5139	1.1262	0.22721	0.82456	0.71742	13505.0	7.5952×10^{-3}	0.079451
2.6263	0.98226	0.32517	0.91468	0.86045	14290.0	8.9881×10^{-3}	0.054310
2.7108	0.88397	0.40459	0.96192	0.93302	14688.0	0.010151	0.044337
2.7833	0.83513	0.47527	0.98440	0.96909	14886.0	0.011204	0.039804
2.8504	0.81156	0.54165	0.99419	0.98650	14982.0	0.012203	0.037712
2.9150	0.80033	0.60603	0.99805	0.99449	15026.0	0.013177	0.036887
2.9787	0.79538	0.66968	0.99941	0.99791	15045.0	0.014142	0.036573
3.0421	0.79342	0.73302	0.99984	0.99927	15053.0	0.015104	0.036448
3.1063	0.79269	0.79726	0.99996	0.99977	15056.0	0.016080	0.036402
3.1695	0.79245	0.86044	0.99999	0.99993	15057.0	0.017040	0.036387
3.2327	0.79238	0.92360	1.0	0.99998	15057.0	0.01800	0.036383
3.2856	0.79236	0.97657	1.0	1.0	15057.0	0.018805	0.036381

TABLE VI (Concl'd)

(d) V_∞ = 60,000 ft/sec

η	Pr	f	f_η	g	T	Y	N
0	0.7000	-0.5000	0	1.8010×10^{-3}	299.81	0	1.0
0.23141	0.69581	-0.49849	0.014205	6.9473×10^{-3}	1096.9	4.6857×10^{-5}	0.65918
0.76059	0.56375	-0.47794	0.068460	0.026231	3076.3	3.9744×10^{-4}	0.45168
1.0437	0.62482	-0.45301	0.10919	0.040992	3766.4	7.0911×10^{-4}	0.40780
1.5141	0.56122	-0.38184	0.19883	0.079991	5722.2	1.5192×10^{-3}	0.33213
1.8562	0.64078	-0.29986	0.28343	0.12217	6549.9	2.3797×10^{-3}	0.29516
2.2011	0.84630	-0.18433	0.39045	0.19725	7483.5	3.5310×10^{-3}	0.26366
2.4727	0.97240	-0.064145	0.49890	0.29833	10227.0	4.8777×10^{-3}	[illegible]
2.7479	1.0203	0.09559	0.69283	0.57812	14137.0	7.2491×10^{-3}	0.058411
2.8465	0.68012	0.17002	0.82330	0.74821	15496.0	8.5460×10^{-3}	0.029648
2.9055	0.49879	0.22109	0.90501	0.83765	16266.0	9.4735×10^{-3}	0.020799
2.9516	0.39778	0.26399	0.95350	0.89083	16782.0	0.10247	0.017085
2.9908	0.33649	0.30191	0.97901	0.92445	17152.0	0.010931	0.0150791
3.0264	0.29855	0.33701	0.99123	0.94717	17463.0	0.011655	0.013980
3.0598	0.27193	0.37021	0.99660	0.96311	17681.0	0.012303	0.013242
3.0917	0.25279	0.40201	0.99878	0.97456	17838.0	0.012934	0.0127[illegible]1
3.1225	0.23882	0.43277	0.99959	0.98292	17952.0	0.013532	0.0123[illegible]9
3.1525	0.22973	0.46291	0.99987	0.98909	18048.0	0.014161	0.012130
3.1821	0.22413	0.49244	0.99997	0.99370	18131.0	0.014766	0.011597
3.2115	0.21995	0.52179	0.99999	0.99714	18193.0	0.015369	0.011199
3.2272	0.21816	0.53754	1.0	0.99861	18220.0	0.015603	0.011358
3.2448	0.21647	0.55508	1.0	1.0	18245.0	0.016056	0.11819

TABLE VII

BOUNDRY LAYER PROFILES FOR EQUILIBRIUM AIR
WITH $f_w = -1.0$ at $P_1 = 1$ atm, $\beta/2 = 0.5$, $j = 0$

(a) $V_\infty = 30,000$ FT/SEC

η	Pr	f	f_η	g	T	Y	N
0.	0.70	-1.0	0.0	7.20×10^{-3}	299.64	0.0	1.0
0.22236	0.70	-0.99937	5.7862×10^{-3}	7.9174×10^{-3}	329.23	2.9799×10^{-5}	0.94968
0.63112	0.70	-0.99451	0.018391	9.7817×10^{-3}	406.21	9.4020×10^{-5}	0.83863
0.95595	0.70	-0.98645	0.031453	0.011976	494.60	1.560×10^{-4}	0.78298
1.3183	0.70	-0.97185	0.050140	0.015678	643.31	2.4230×10^{-4}	0.69393
1.6165	0.69968	-0.95405	0.069755	0.020169	815.99	3.3591×10^{-4}	0.68402
1.9153	0.69392	-0.92990	0.092443	0.026156	1038.4	4.5417×10^{-4}	0.67365
2.2205	0.69531	-0.89755	0.12055	0.034874	1343.6	6.0840×10^{-4}	0.61232
2.6134	0.70924	-0.84149	0.16766	0.053044	1974.6	8.7993×10^{-4}	0.53651
3.0086	0.58802	-0.76333	0.22996	0.081467	2693.0	1.2762×10^{-3}	0.48041
3.3327	0.56809	-0.67888	0.29321	0.11371	3197.1	1.6955×10^{-3}	0.44286
3.6858	0.63618	-0.56095	0.37810	0.16706	3832.5	2.2616×10^{-3}	0.40751
3.9936	0.60935	-0.43108	0.46932	0.24166	4897.6	2.9171×10^{-3}	0.35861
4.2043	0.55758	-0.32462	0.54168	0.30234	5592.1	3.4999×10^{-3}	0.33683
4.5289	0.60181	-0.12984	0.63954	0.41767	6269.0	4.5853×10^{-3}	0.30873
4.8270	0.69017	-0.083234	0.76967	0.55665	6778.6	5.7915×10^{-3}	0.28427
5.1519	0.80746	0.35161	0.87921	0.73450	7310.1	7.3766×10^{-3}	0.26031
5.4583	0.88020	0.63284	0.95091	0.87881	7784.9	9.1131×10^{-3}	0.24187
5.7415	0.89378	0.90765	0.98485	0.95816	8271.1	0.010979	0.23320
6.0191	0.88554	1.1830	0.99651	0.98874	8511.5	0.012930	0.23116
6.2602	0.88277	1.4237	0.99926	0.99710	8580.8	0.014659	0.23040
6.5096	0.88199	1.6730	0.99989	0.99943	8600.3	0.016457	0.23020
6.7982	0.88182	1.9616	1.0	0.99994	8604.6	0.18542	0.23016
7.0038	0.88180	2.1671	1.0	0.99999	8605.1	0.020027	0.23015
7.1349	0.88180	2.2983	1.0	1.0	8605.1	0.020974	0.23015

TABLE VII (Cont'd)

(G) V_∞ =40,000 FT/SEC

η	Pr	f	f_η	g	T	Y	N
0.0	0.70	-1.0	0.0	4.10×10^{-3}	303.31	0.0	1.0
0.23837	0.70	-0.99968	2.6857×10^{-3}	4.2081×10^{-3}	311.30	2.7001×10^{-5}	0.98578
0.68467	0.70	-0.99543	1.0662×10^{-2}	4.6380×10^{-3}	342.94	1.0475×10^{-4}	0.93530
1.5118	0.70	-0.98595	1.9908×10^{-2}	5.3551×10^{-3}	396.28	1.9017×10^{-4}	0.84783
2.2020	0.70	-0.96786	3.3157×10^{-3}	6.8306×10^{-3}	502.53	3.0315×10^{-4}	0.78238
2.7135	0.70	-0.94760	4.6898×10^{-2}	8.8789×10^{-3}	649.51	4.0951×10^{-4}	0.69706
3.2579	0.69780	-0.91685	6.6895×10^{-2}	1.2699×10^{-2}	909.90	5.6552×10^{-4}	0.68920
3.7234	0.69550	-0.88085	8.8810×10^{-2}	1.8060×10^{-2}	1252.3	7.4957×10^{-4}	0.63154
4.1389	0.70252	-0.83873	0.11524	2.6278×10^{-2}	1750.8	9.7608×10^{-4}	0.56179
4.5092	0.62378	-0.79053	0.14633	3.8240×10^{-2}	2410.5	1.2596×10^{-3}	0.50672
4.9902	0.56548	-0.70804	0.19933	6.0783×10^{-2}	3124.3	1.7602×10^{-3}	0.45110
5.3716	0.61320	-0.62184	0.25541	9.0026×10^{-2}	3698.9	2.2747×10^{-3}	0.40999
5.7097	0.60937	-0.52504	0.32040	0.13434	4869.1	2.8824×10^{-3}	0.36246
6.003	0.56276	-0.42187	0.39183	0.18412	5777.3	3.5953×10^{-3}	0.33206
6.3338	0.62867	-0.27513	0.49182	0.26516	6489.1	4.6201×10^{-3}	0.29983
6.6537	0.77950	-2.9358×10^{-2}	0.61159	0.38899	7185.3	5.8655×10^{-3}	0.26679
6.9045	0.89686	6.7517×10^{-2}	0.72142	0.53073	8100.6	7.1131×10^{-3}	0.23582
7.2152	1.1098	0.31358	0.86143	0.74072	11,150.	9.3483×10^{-3}	0.17600
7.5006	1.2024	0.57549	0.96338	0.93736	12,528.	1.2163×10^{-2}	0.11986
7.7749	1.2011	0.84538	0.99570	0.99427	12,780.	1.5201×10^{-2}	0.10817
7.9505	1.2010	1.0205	0.99924	0.99922	12,800.	1.7186×10^{-2}	0.10721
8.1278	1.2010	1.1979	0.99988	0.99993	12,803.	1.9196×10^{-2}	0.10707
8.2692	1.2010	1.3392	0.99998	0.99999	12,804.	2.0798×10^{-2}	0.10705
8.3385	1.2010	1.4086	1.0	1.0	12,804.	2.1584×10^{-2}	0.10706

TABLE VII (Concl'd)

(c) V_∞ = 50,000 ft/sec

η	Pr	f	f_η	g	T	Y	N
0.0	0.70	-1.0	0.0	2.60×10^{-3}	300.56	0.0	1.0
0.30557	0.70	-0.99969	2.0486×10^{-3}	2.6163×10^{-3}	302.19	3.0646×10^{-5}	0.9970
0.77874	0.70	-0.99796	5.2582×10^{-3}	2.6505×10^{-3}	305.54	7.85×10^{-5}	0.99079
1.6143	0.70	-0.99115	1.1093×10^{-2}	2.7485×10^{-3}	315.48	1.6477×10^{-4}	0.97367
2.2695	0.70	-0.98232	$1.5[illegible]0\times10^{-2}$	2.8812×10^{-3}	328.78	2.3498×10^{-4}	0.95200
2.8755	0.70	-0.97123	2.0731×10^{-2}	3.0797×10^{-3}	348.64	3.0330×10^{-4}	0.92244
3.4890	0.70	-0.95688	2.6179×10^{-2}	3.4079×10^{-3}	381.37	3.7789×10^{-4}	0.88021
3.9795	0.70	-0.94282	3.1277×10^{-2}	3.8321×10^{-3}	423.82	4.4454×10^{-4}	0.83114
4.4765	0.70	-0.92581	3.7375×10^{-2}	4.4973×10^{-3}	489.13	5.1923×10^{-4}	0.78831
4.9866	0.70	-0.90480	4.5419×10^{-2}	5.6218×10^{-3}	599.46	6.0956×10^{-4}	0.70671
5.6643	0.69879	-0.86916	6.063×10^{-2}	8.4001×10^{-3}	860.56	7.7290×10^{-4}	0.68562
6.3618	0.69532	-0.81966	8.2867×10^{-2}	1.3881×10^{-2}	1338.3	1.0230×10^{-3}	0.61415
6.7960	0.7059.	-0.77953	0.10311	2.0373×10^{-2}	1863.6	1.2511×10^{-3}	0.54525
7.2009	0.60058	-0.73284	0.12860	2.9949×10^{-2}	2550.2	1.5504×10^{-3}	0.49267
7.6766	0.56865	-0.66264	0.16862	4.6259×10^{-2}	3212.4	2.0183×10^{-3}	0.44251
7.9958	0.57892	-0.60346	0.20376	6.3318×10^{-2}	3497.9	2.4115×10^{-3}	0.39495
8.2919	0.64649	-0.53723	0.24488	8.8349×10^{-2}	4618.3	2.8665×10^{-3}	0.37457
8.5912	0.55789	-0.45623	0.29852	0.12183	5603.4	3.4883×10^{-3}	0.33701
8.8878	0.60054	-0.35828	0.36431	0.16625	6258.6	4.2601×10^{-3}	0.30973
9.2446	0.74304	-0.21094	0.46690	0.25239	7022.5	5.4293×10^{-3}	0.27267
9.6850	0.94587	3.1450×10^{-2}	0.64410	0.45225	10,057.	7.6009×10^{-3}	0.20833
9.9947	1.1116	0.25852	0.84028	0.76919	13,606.	1.0423×10^{-2}	7.5786×10^{-2}
10.065	1.0340	0.31996	0.89477	0.85261	14,081	1.1289×10^{-2}	6.0055×10^{-2}
10.30	0.82136	0.54384	0.99047	0.98632	14,942.	1.4582×10^{-2}	3.8574×10^{-2}
10.471	0.79499	0.71380	0.99885	0.99898	15,047.	1.7155×10^{-2}	3.6548×10^{-2}
10.630	0.79236	0.87350	0.99999	1.0	15,057	1.9582×10^{-2}	3.6381×10^{-2}

V. CONCLUSIONS

1. Discrepancies between experiment and theory have been significantly reduced both by an improvement in Yos' predictions and also by a further refinement in the data reduction from arc experiments.

2. The heat transfer rate to the wall is strongly affected by the shape and the occurance of the dip in the graph of thermal conductivity versus temperature.

3. Good agreement between theory and experiment has been obtained for equilibrium air for flight velocities up to 55,000 ft/sec; for equilibrium nitrogen agreement between theory and experiment is excellent up to flight velocities of 50,000 ft/sec.

VI. REFERENCES

1. Adams, M., A Look at the Heat Transfer Problem at Super Satellite Speeds, Presented at the ARS 15th Annual Meeting (December 1960).

2. Van Tassell, W., and A. J. Pallone, Similar Solutions of the Compressible Laminar Boundary Layer Equations for Air in Equilibrium Dissociation and Ionization With and Without Air Injection in the Stagnation Region, Avco RAD-TM-61-22 (June 1961).

3. Hansen, C. F., Approximations for the Thermodynamic and Transport Properties of High Temperature Air, NACA TN 4150 (March 1958).

4. Cohen, N. B., Boundary Layer Similar Solutions and Correlation Equations for Laminar Heat Transfer Distribution in Equilibrium Air at Velocities up to 41,000 feet per second, NASA TR-R-118 (1961).

5. Scala, S. M., Heating Problems of Entry into Planetary Atmospheres from Supercircular Orbiting Velocities, Proceedings of Symposium on Aerothermo-Elasticity, ASD Tech. Rep. No. 61-645, pp. 531-591 (November 1961).

6. Pallone, A. J., and W. Van Tassell, Effects of Ionization on Stagnation-Point Heat Transfer, Phys. of Fl. (July 1963).

7. Yos, J. M., Transport Properties of Nitrogen, Hydrogen, Oxygen, and Air to 30,000°K, RAD-TM-63-7. Avco Research and Advanced Development Division, Wilmington, Mass. (March 1963).

8. Hoshizaki, H., Heat Transfer in Planetary Atmospheres at Supersatellite Speeds, ARS Journal, pp. 1544-51 (October 1962).

9. Fay, J. A., and N. H. Kemp., Theory of Stagnation-Point Heat Transfer in a Partially Ionized Diatomic Gas, AERL Research Report 144, Avco Everett Research Lab (April 1963).

10. Rose, P. H., and J. O. Stankevics, Heat Transfer Measurements in Partially Ionized Air Utilizing Infrared Heat Transfer Gages, Presented at AIAA Entry Technology Conference, AERL Research Report 196 (October 1964).

11. Howe, J. T., and Y. S. Shaeffer, Effects of Uncertainties in the Thermal Condictivity of Air on Convective Heat Transfer For Stagnation Temperature up to 30,000°K, NASA TN D-2678 (February 1965).

12. Bennett, S., J. M. Yos, C. F. Knopp, J. Morris, and W. L. Bade, Theoretical and Experimental Studies of High-Temperature Gas Transport Properties, Final Report, RAD-TR-65-7 (May 1965). (See also RAD-SR-65-35, February 1965).

13. Weisblatt, H., and G. H. Rushton, Private Communication (August 1964)

14. Reshotko, E., and C. B. Cohen, Heat Transfer at the Forward Stagnation Point of Blunt Bodies, NACA TN 3513 (July 1955).

15. Libby, P., The Homogeneous Boundary Layer at an Axisymmetric Stagnation Point With Large Rates of Injection, PIBAL Report No. 605, Polytechnic Institute of Brooklyn (August 1959).

16. Howe, J. T., and Y. S. Sheaffer, Effects of Uncertainties in the Thermal Conductivity of Air on Convective Heat Transfer for Stagnation Temperature up to 30,000°K, NASA TN D-2678 (February 1965).

17. Howe, J. T., and J. R. Viegas, Solutions of the Ionized Radiating Shock Layer, Including Reabsorption and Foreign Species Effects, and Stagnation Region Heat Transfer, NASA TR R-159 (1963).

18. Fay, J. A., Entry Heat Transfer at Super-Orbital Speeds, Fluid Mechanics Laboratory Publication No. 64-7 Dept. of Mech. Engrg., MIT, Cambridge, Mass. (August 1964).

19. Maecker, H., Zeitschr. Phys., 141, No. 1/2, 98 (1955).

20. Hayes, W. D and R. F. Probstein, Hypersonic Flow Theory, Academic Press, pp. 155, 239 (1959).

21. Korkan, K. D., Stagnation Point Velocity Gradient on Two-Dimensional and Axisymmetric Bodies in Hypersonic Flow, ARS Journal, p. 1942 (December 1962).

Unclassified

Security Classification

DOCUMENT CONTROL DATA - R&D

(Security classification of title, body of abstract and indexing annotation must be entered when the overall report is classified)

1. ORIGINATING ACTIVITY (Corporate author) Avco Corp., Research and Development Division 201 Lowell Street Wilmington, Massachusetts	2a. REPORT SECURITY CLASSIFICATION Unclassified 2b. GROUP

3. REPORT TITLE

Convective Stagnation Point Heating for Reentry Speeds up to 70,000 Feet/Second Including Effects of Large Blowing Rates (Task 3.1: Flowfield Analysis -- REST Program)

4. DESCRIPTIVE NOTES (Type of report and inclusive dates)

Technical Memorandum

5. AUTHOR(S) (Last name, first name, initial)

DeRienzo, P., Pallone, A.

6. REPORT DATE	7a. TOTAL NO. OF PAGES	7b. NO. OF REFS
5 January 1965	60	71

8a. CONTRACT OR GRANT NO. AF04(694)-498 b. PROJECT NO. c. d.	9a. ORIGINATOR'S REPORT NUMBER(S) RAD-TM-65-58 9b. OTHER REPORT NO(S) (Any other numbers that may be assigned this report)

10. AVAILABILITY/LIMITATION NOTICES

None

11. SUPPLEMENTARY NOTES	12. SPONSORING MILITARY ACTIVITY
None	BSD

13. ABSTRACT

The current state-of-the-art is reviewed with respect to the calculation of convective stagnation point heating at supersatellite reentry speeds. Recently calculated transport properties have been compared with experiment. It is noted that theoretical and experimental estimates of the total thermal conductivity are in much closer agreement than reported by earlier investigators.

Similarity solutions employing these recently computed transport properties are presented for the convective heat transfer rate in an ionized, dissociated gas for equilibrium air and equilibrium nitrogen at reentry speeds up to 70,000 feet/sec. Solutions are also obtained for the case when large rates of injection are introduced at the stagnation point. Tables of boundary layer characteristics including profiles of temperature, velocity, and enthalpy are presented for the axisymmetric and two-dimensional stagnation point.

This task was initiated under the REST Program under the cognizance of Air Force Ballistic Systems Division; the major portion of the work, however, has been company supported.

DD FORM 1 JAN 64 1473

Unclassified

Security Classification

Unclassified
Security Classification

14. KEY WORDS	LINK A		LINK B		LINK C	
	ROLE	WT	ROLE	WT	ROLE	WT
1. Reentry Speeds						
2. Supersatellite Velocities						
3. Transport and Thermodynamic Properties						
4. Body Geometry						
5. Ablating Surface						
6. Heat Transfer Rate						
7. Thermal Conductivity						
8. Ionization						

INSTRUCTIONS

1. ORIGINATING ACTIVITY: Enter the name and address of the contractor, subcontractor, grantee, Department of Defense activity or other organization (corporate author) issuing the report.

2a. REPORT SECURITY CLASSIFICATION: Enter the overall security classification of the report. Indicate whether "Restricted Data" is included. Marking is to be in accordance with appropriate security regulations.

2b. GROUP: Automatic downgrading is specified in DoD Directive 5200.10 and Armed Forces Industrial Manual. Enter the group number. Also, when applicable, show that optional markings have been used for Group 3 and Group 4 as authorized.

3. REPORT TITLE: Enter the complete report title in all capital letters. Titles in all cases should be unclassified. If a meaningful title cannot be selected without classification, show title classification in all capitals in parenthesis immediately following the title.

4. DESCRIPTIVE NOTES: If appropriate, enter the type of report, e.g., interim, progress, summary, annual, or final. Give the inclusive dates when a specific reporting period is covered.

5. AUTHOR(S): Enter the name(s) of author(s) as shown on or in the report. Enter last name, first name, middle initial. If military, show rank and branch of service. The name of the principal author is an absolute minimum requirement.

6. REPORT DATE: Enter the date of the report as day, month, year; or month, year. If more than one date appears on the report, use date of publication.

7a. TOTAL NUMBER OF PAGES: The total page count should follow normal pagination procedures, i.e., enter the number of pages containing information.

7b. NUMBER OF REFERENCES: Enter the total number of references cited in the report.

8a. CONTRACT OR GRANT NUMBER: If appropriate, enter the applicable number of the contract or grant under which the report was written.

8b, 8c, & 8d. PROJECT NUMBER: Enter the appropriate military department identification, such as project number, subproject number, system numbers, task number, etc.

9a. ORIGINATOR'S REPORT NUMBER(S): Enter the official report number by which the document will be identified and controlled by the originating activity. This number must be unique to this report.

9b. OTHER REPORT NUMBER(S): If the report has been assigned any other report numbers *(either by the originator or by the sponsor)*, also enter this number(s).

10. AVAILABILITY/LIMITATION NOTICES: Enter any limitations on further dissemination of the report, other than those imposed by security classification, using standard statements such as:

(1) "Qualified requesters may obtain copies of this report from DDC."

(2) "Foreign announcement and dissemination of this report by DDC is not authorized."

(3) "U. S. Government agencies may obtain copies of this report directly from DDC. Other qualified DDC users shall request through ______."

(4) "U. S. military agencies may obtain copies of this report directly from DDC. Other qualified users shall request through ______."

(5) "All distribution of this report is controlled. Qualified DDC users shall request through ______."

If the report has been furnished to the Office of Technical Services, Department of Commerce, for sale to the public, indicate this fact and enter the price, if known.

11. SUPPLEMENTARY NOTES: Use for additional explanatory notes.

12. SPONSORING MILITARY ACTIVITY: Enter the name of the departmental project office or laboratory sponsoring *(paying for)* the research and development. Include address.

13. ABSTRACT: Enter an abstract giving a brief and factual summary of the document indicative of the report, even though it may also appear elsewhere in the body of the technical report. If additional space is required, a continuation sheet shall be attached.

It is highly desirable that the abstract of classified reports be unclassified. Each paragraph of the abstract shall end with an indication of the military security classification of the information in the paragraph, represented as *(TS), (S), (C), or (U)*.

There is no limitation on the length of the abstract. However, the suggested length is from 150 to 225 words.

14. KEY WORDS: Key words are technically meaningful terms or short phrases that characterize a report and may be used as index entries for cataloging the report. Key words must be selected so that no security classification is required. Identifiers, such as equipment model designation, trade name, military project code name, geographic location, may be used as key words but will be followed by an indication of technical context. The assignment of links, rules, and weights is optional.

Unclassified
Security Classification